Final Report

"Cycloidal Propulsion for UAV VTOL Applications"

for

SBIR Topic Number N98-022

Contract Number: N68335-98-C-0120 / Item 0001AF

Reporting Period October 1 - 31, 1998

Prepared For:

Government Technical Liaison

Naval Air Warfare Center - Aircraft Division

Attn: W. Parsons - Code AIR 441

48142 Shaw Road - Unit 5

Patuxent River, Maryland 20670-1906

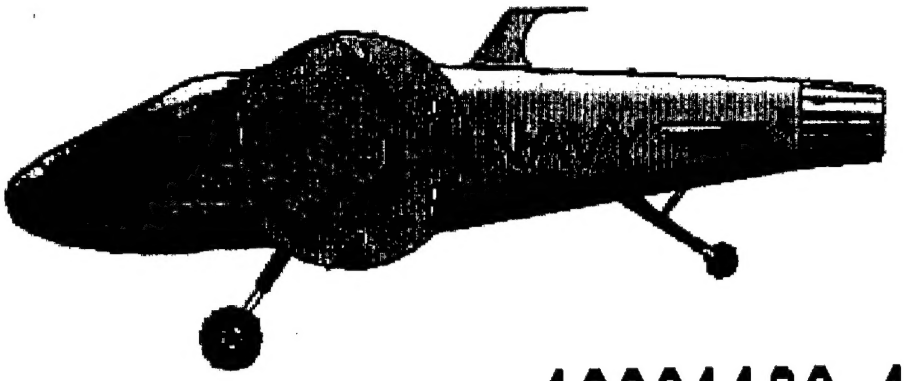

Prepared By:

BOSCH Aerospace, Inc.

James H. Boschma, Technical Director

7501 South Memorial Parkway, Suite 207

Huntsville, Alabama 35802-2226

15 November 1998

Distribution Unlimited

FOREWORD

This report is prepared for Contract Number N68335-98-C-0120 as CLIN 0001AF Final Report for the reporting period October 1-31, 1998 under SBIR Topic N98-022 entitled "Cycloidal Propulsion for UAV VTOL Applications."

This report is prepared by BOSCH Aerospace, Inc., James H. Boschma, Principal Investigator for this project, and Callum Sullivan, Design Engineer.

BOSCH AEROSPACE, INC.
JUDITH L. BOSCHMA, PRESIDENT
JAMES H. BOSCHMA, TECHNICAL DIRECTOR
7501 South Memorial Parkway, Suite 207
Huntsville, Alabama 35802-2226
phone: (256) 882-9394 fax: (256) 883-2951

CONTENTS

FIGURES

Executive Summary

BOSCH Aerospace, Inc., (BOSCH Aerospace) and subcontractor MSU RASPET Flight Research Laboratory (RASPET) accomplished successful development and testing of a prototype Curtate Cycloidal Propeller during the SBIR Phase I effort which concluded on October 31, 1998. This propulsion concept holds significant promise for adaptation to UAV VTOL operations. Thrust levels demonstrated were substantially higher than achievable by the best screw-type propellers, and approximately equal to those of high-end helicopters. Vectoring of thrust through a 360° arc, and low-noise characteristics throughout the RPM range were demonstrated. Also accomplished was identification of efficiency gain techniques that may increase the overall thrust by approximately 30%.

A literature search and study of cycloidal propeller testing conducted by Boeing Corporation and U.S. Government agencies between 1920 and 1945 were essential elements of Phase I. A computer model based upon this historical data was developed to allow aerodynamic performance assessment of candidate designs. The model was incorporated into the System Engineering effort where potential designs for the Navy UAV VTOL requirements were examined, and the optimum design identified. The Curtate Cycloid design provides the best hover performance, and excellent flight performance to speeds of approximately 120 knots. The BOSCH Aerospace team selected a full-scale (four-foot diameter) design. After consulting with the Navy technical monitor, the design was optimized, materials selected, and fabrication tolerances defined.

Because the Cycloidal propeller is unique, no existing test facility or test fixtures existed. Thus, we designed and fabricated a test fixture specifically suited for testing this prototype, as well as future cycloidal propeller designs. Components were function tested on CAD, then manufactured before final assembly in Huntsville. During assembly, two five-foot diameter polycarbonate (lexan) disks, which were designed to eliminate flow turbulence near the center of the blade sections, arrived late and were found to be defective. Due to time constraints, these disks were left out of the prototype. The resulting assembly was function tested, dynamically balanced, and moved to the RASPET facility for instrumentation and tests.

The cycloidal propeller tests were designed to accomplish two major goals, to measure thrust, and to assess thrust vector capability. Several concurrent objectives were also sought, noise assessment, educating the research team on operating characteristics of a Cycloidal propeller, examination of the prototype's mechanical performance, identification of potential design improvements, and assessment of the test fixture for future use.

Thrust measurements were taken at various RPMs in two orientations, 90° up, and then 90° down from horizontal. Vector assessment was made throughout the 360° arc. Downward thrust was approximately 20% below projections. Upward thrust in lower RPM ranges was 3% above projections. However, as RPM increased thrust decreased to the 20% below projections level. Reduced data showed that thrust varied from approximately 10.88 *lb./Hp* at low RPM, to 8.4 *lb./Hp* at high RPM. A probable solution to eliminate this anomaly was identified.

The Phase I prototype test results showed outstanding thrust levels, clear vector control with highly defined flow fields, and whisper-quiet operations. When comparing the performance demonstrated by the prototype to modern military VTOL systems (UH-60 helicopter at *6.4 lb./Hp*, V-22 Tilt Wing Aircraft at *4.9 lb./Hp.*), the potential for Cycloidal propulsion for UAV VTOL application becomes strikingly apparent.

1.0 Introduction and Background

The cycloidal propeller, which can be described as a horizontal rotary wing, offers powerful thrust levels, and a unique ability to change the direction of that thrust almost instantly. The cycloidal propeller is the most efficient form of propeller conceived to date, and was recognized as the solution to overcome propulsion deficiencies associated with airships. This concept was studied and tested by the Boeing Company and the U.S. Navy in the 1920s for adaptation to rigid airships.

The U.S. Navy airship Shenandoah was scheduled to be the first flight vehicle to be equipped with this new cycloidal propulsion system. Plans had been drawn and preparations were being made to modify the airship by outfitting it with cycloidal propellers. However, in the early hours of September 3, 1925 the Shenandoah broke up in flight and crashed. Unfortunately, the loss of the Shenandoah also marked the loss of opportunity to place a cycloidal propeller into flight operation.

Two other airships, the Akron and her sister ship the Macon, were not in service for another eight years. However, neither of these machines benefited from the control advantages of the new propulsion system. By that time, the Goodyear Rubber Company had joined with Zeppelin of Germany, a company that had seen much success with conventional airscrews, and the decision by Goodyear/Zeppelin not to pursue this new technology meant that a second opportunity was lost to show the efficiency of the cycloidal propeller.

Following the loss of these two airships, and the subsequent destruction of the Hindenburg, interest in airships virtually disappeared. Conventional aircraft continued to develop, and with the advent of the turbine engine, conventional air travel was revolutionized. However, to this day no rotary-winged aircraft has been developed that can match the efficiency of a cycloidal propeller. The latest in VTOL aircraft, the V-22 Osprey, falls well *below* the closest rival to cycloidal systems, the MD-500 (Figure 1).

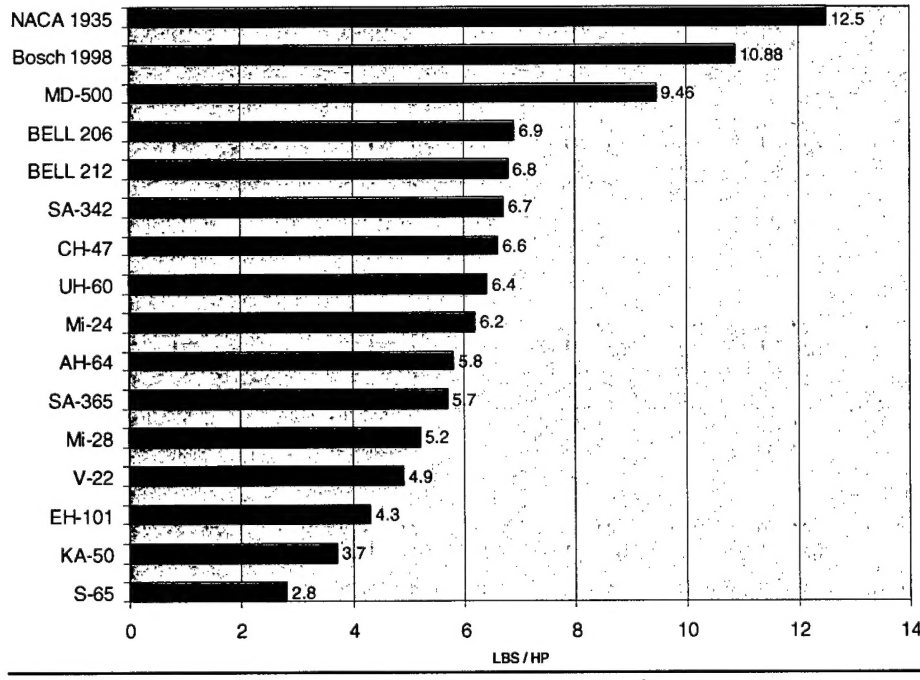

Figure 1. Thrust Comparison Chart

This chart provides a comparison to wind tunnel data from cycloidal propellers and a selection of the most modern rotary winged aircraft in service in the world today including many Soviet-built machines. (data from Jane's All the World Aircraft)

2.0 Design Specifications

A design specification is the cornerstone of any product, and the reference from which all research is based and all development steps attempt to meet. This is often referred to as the Product Design Specification (PDS). This 18-point comprehensive specification was required by the BOSCH Aerospace design team to expedite the design and manufacturing process for a successful product.

The main goal of this Phase I research was to evaluate the potential of a cycloidal propulsion system for VTOL vehicles. This phase of the research did not require a complete and marketable vehicle. Consequently, we were concerned with only four aspects of the design: weight, performance, cost, and time.

Based upon previous experience with UAVs, Mr. Christopher Veith of the Naval Warfare Center, Aircraft Division, recommended the following guideline specifications for the Phase I effort:

- Weight 600 pounds gross, including fuel and payload
- Speed From Hover to 120 knots plus
- Range 150 miles operational radius
- Capabilities Hover and flight at 4,000 feet MSL at 95° F

To meet these specifications, the major obstacle that presented itself was an aerodynamic one:

- Number of blades
- Section of blades
- Chord and aspect ratio of blades
- Blade speed and diameter of rotation
- Angle of attack of blades
- Thrust dwell angle
- Rotational speed of blade group
- Down wash and turbulent interference

All of the factors listed above were variables in the one equation that determined the best lift and thrust compromise to enable the cycloidal propeller to function effectively. This was the aerodynamic task assigned to the RASPET group. Using a computer model, RASPET engineers conducted tests to determine blade configurations within the parameters of fixed data inputs. Such limiting factors included the diameter of the rotating disk, which if left to the computer might suggest the largest possible dimension to maximize efficiency.

In conjunction with this, there was the question of systems control and mechanical structures. The blades required the correct mounting and degrees of motion to obtain the aerodynamic requirements outlined by the findings of RASPET. It was possible that a blade configuration could be devised that was too efficient, and that mechanical loads would be in excess of mechanical materials capabilities. Therefore, the two systems were worked in close cooperation with each other for realistic results. (Again, one of the fixed variables could be related to materials optimization.)

With aerodynamics and mechanics comes the question of control. Since this will be a UAV, and not in line-of-sight for the majority of flight operations, stability and ease of control are factors. A cycloidal system is not expected to be as unstable and difficult to control as an R/C helicopter in the hover. In forward flight, it has the option of being able to concentrate thrust purely in the forward direction and be reliant on more traditional means of lift, such as in an AV8 Harrier. It was the intent of the BOSCH Aerospace research team to add complexity *only* 'if and when' a simple solution could not be found.

A suitable power plant was required to be light, fuel efficient, and powerful due to the relatively low weight of the unloaded aircraft. Norton motorcycle engines are Wankel rotary-type and benefit from having few moving parts, being exceptionally smooth, and are available in various stages of tune-up to 150 Hp. Other power sources were also considered. Early estimations suggested that the thrust required per lifting blade would be in the region of 375 pounds. In 1923, Kirsten's experiments showed that a cycloidal propeller is capable of 12.6 pounds from one horsepower.

From previous works evaluated during our literature search, it was found that of the two distinctive forms of the cycloidal system, low-pitch and high-pitch, the low-pitch was best suited to hovering and low airspeeds of up to 60 MPH (where it is most efficient). Higher speeds, though capable in the low-pitch mode, are better suited to the more slipstreamed and more complex high-pitch system. Combining the two into a universal cycloid is the ultimate efficiency answer to providing a wide range of airspeeds. The expected mechanisms and microchip control technology required for universal motion is expected to be complicated and mechanically demanding. *When* these steps to the ultimate efficiency propeller are to be taken, will be determined by the low-pitch test results.

At this point, decisions were made by the research team and certain variables became fixed ones to reduce the complexity of the computations. Fifteen-foot diameter blade groups worked well and produced excellent data with Wheatley in 1935. Our objective was to reproduce these figures with a four-foot diameter blade group. This diameter restriction decision was based purely on the expected physical limitations of a shipboard UAV.

With vertical thrust, there comes a point in the rotation where a blade is at top dead center (TDC) and assumes an angle of attack (AoA) at 15° to generate vertical lift. The opposing blade is also assuming a positive AoA of 15° at bottom dead center (BDC). However, the blade at TDC is generating vertical lift considerably more effectively that the one at BDC due to several considerations. One reason is the top blade is rotating in a positive direction and is assuming a positive AoA in a relatively clean airflow. The blade at BDC is assuming a positive AoA while still rotating in a negative direction into disturbed air generated by the top blades' downwash. Consequently the bottom blade should assume a relatively greater AoA to generate complementary lift. This cannot be done with a fully symmetrical system using a single common blade point. To overcome this, the mechanical common center must be replaced by a non-linear system such as a cam or other electronic device. These refinements should be considered in future development.

The disturbed air generated by the leading blade could alter the computed optimum angle of attack, so a wider range of test angles was incorporated into the test fixture so that the blades could be tested at up to 45°.

Although not following the theoretically better non-symmetrical blade path, it should be noted that the computed data of the basic low-pitch cycloidal propeller looks very promising and stands as a solid platform for future refinement.

2.1 Blade Configuration

The traditional means of supporting the blades in a horizontal rotary wing configuration has been in the form of a cantilever where the blade is supported by the root. This requires a large and substantial root hub to support the long moment arm of the loaded blade. The configuration we chose employs the blade supported at its center to dramatically reduce loading (Figure 2-page 6). This approach also reduces material required to build the hubs, and therefore saves rotational weight. This layout is in no way detrimental to the aerodynamic performance of the system due to the polycarbonate (lexan) covers fitted (Figure 3).

Our concept design consists of two main blade groups rotating each side of a main fuselage with a third blade group in the tail as an anti-torque device and a means of lateral control in the hover. This would provide the cleanest possible airflow to the blades and thus provide more predictable results. A four-blade group system was considered to eliminate the need for anti-torque devices, but was rejected because of forward airflow complications.

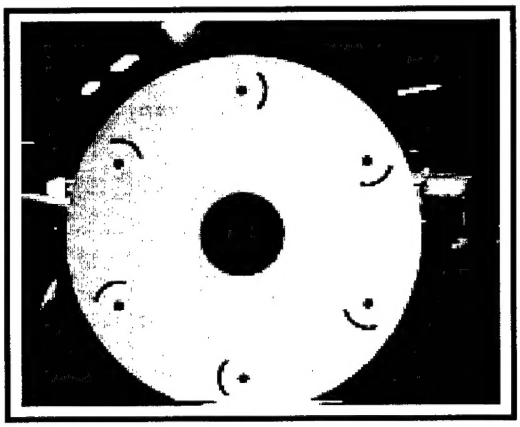

Figure 3. Polycarbonate (lexan) Aero-covers

2.1.1 Mechanical and Control

Two major issues required resolution:
- Providing control to the blades enabling them to follow the aerodynamic model, and
- Providing power and control to the blade group.

2.1.2 Blade Control

A simple 1:2 scale model was constructed to aid in the understanding of required blade motion (Figure 4). Such models are important in the comprehension of the cycloidal movement, as it is difficult to visualize multiple varying blade angles while they are rotating.

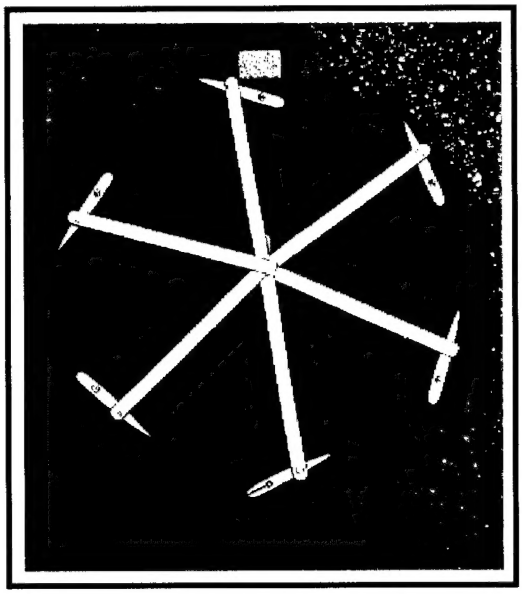

Figure 4. Model of required blade motion

Several options were available to us that could not be conceived in previous purely mechanical experiments:

a. Servos / electrical / mechanical.
b. Hydraulics / electrical / mechanical.
c. Pneumatic / hydraulic actuators / electrical.
d. Purely mechanical.

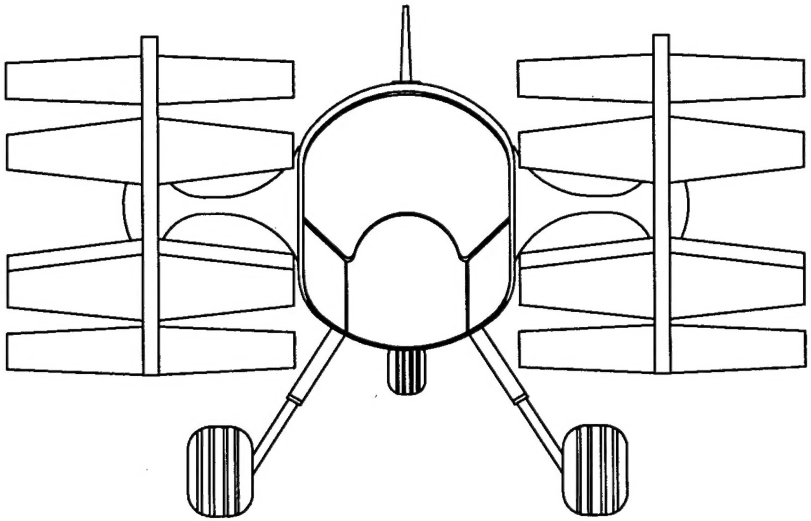

Center Blade configuration

low bending loads

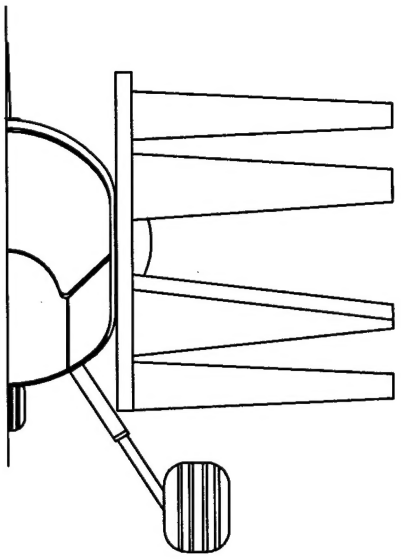

Cantilever configuration

High bending loads

Figure 2

2.1.2.a Servos. Small electric servomotors in production are implemented by many industries to perform high quality precision work. These are high torque and power units capable of rapid and highly repetitive tasks. For our application, repetition frequency is between 10-20 Hz, which means that rapid movement is required. Such units have multimillion cycle specifications and appear well suited to this application. They would require complex computational control, however, and are outside the initial goals of the Phase I effort. Such a system would be useful for optimum control as each servo could be instructed individually for angle of attack, dwell angle, partial and full feathering. Similar systems to those found on high performance vehicles active suspension units could be utilized in this application. These units are designed to be lightweight and powerful, controlled by microprocessors and are capable of extremely rapid movement. These are ideas worth investigating in a Phase II effort.

2.1.2.b Hydraulics. Hydraulics would be a powerful and potentially compact means of controlling the blade angles in conjunction with stepper motors and electronics. These systems are being investigated as a means of future development for the cycloid unit in addition to the servo approach.

2.1.2.c Pneumatics. Pneumatics are in their nature slow and difficult to predict. They also suffer from their inability to transfer energy efficiently. This application is not suitable for their use.

2.1.2.d Purely Mechanical. The most appealing approach was a mechanical one for its relative simplicity and rugged predictability. For the low-pitch cycloidal system being built for the initial tests, a similar mechanism was devised to incorporate the control features of the model shown. The key to providing this control is the stationary control head located in the center of the blade group. In order to enable a 45° movement, the common link to all the blades must occur at 2.6 inches from the center instead of the 1.5 for the 26° AoA. The center mechanism has a graduated worm-drive scale (the white section shown in Figure 5a and 5b) enabling off-axial movement from the drive shaft up to three (3) inches. In Figure 5a, that would be 3" down. Figure 5b shows the center control carriage behind the red common blade arm location. The master rod linkage, seen at the 7 o'clock position, ensures that the other five control rods do not rotationally lock up as the system is run. This is very similar to radial engine devices.

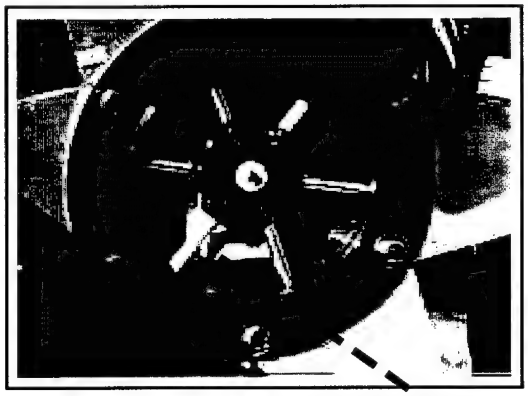

Figure 5a. Center Control Carriage

While in motion, the white control carriage remains stationary, but is able to be moved throughout 360° by the operator via a worm-drive mechanism. Due to the nature of aerodynamics, the maximum vertical lift was not expected to be generated when the blades are at TDC, but occurred a few degrees either side of it. Similar conditions apply throughout the 360° rotation. The central adjustment for blade AoA can also be independently rotated to enable fine-tuning of the thrust direction.

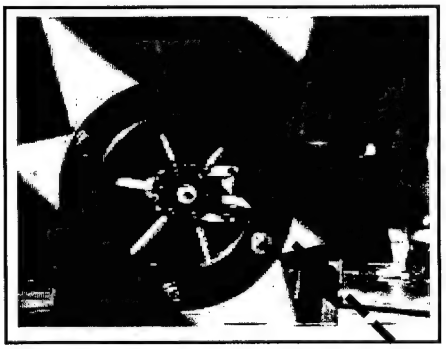

Figure 5b. Control Carriage at 90°

2.2 Blade Construction

All blades for the initial construction were made using an all-metal ribbed and skinned built-up structure. Each rib was CNC or laser cut from a CAD computer file to ensure accuracy, then balanced. Future development may involve the use of tapered sections to reduce tip loading, but as each protruding surface is only two-feet long, this may not be necessary. The test fixture has constant chord blades. Each blade can easily be removed and replaced to enable different sections or non-constant chord airfoils to be tested.

Computer results were generated using a blade group with a common centerpoint where all of the control rods effectively meet. All blades rotate about a common axis, but their angle of attack is determined by a concentric common axis. The individual blade movement is mirrored in motion by its opposite number. This motion appears to be a good approximation of a pure sine, cosine wave.

Most components in this Phase I build are of 6061 T6 origin to save weight and with key structural components of 4130 in the areas of tension of compression. Such key components include the blade main spar that must not bend significantly to minimize aerodynamic losses. Although a full-length spar was originally used to prevent the blades bending, it was cut down in length due to concern about rotational weight. Outside the rotating blade group, construction mainly consisted of mild and hardened steel. In addition to the structural material, two polycarbonate disks were to be positioned on each side of the central disk. During test sessions high-speed film was used to record the system under load, and the use of the Lexan disks would have enabled components such as the blade control rods to be viewed. These disks were also to provide a clean aerodynamic skin to separate rotating mechanisms from the blades. Unfortunately, these disks arrived defective, and due to time constraints were not utilized in testing. During the Phase I Option period these disks will be repaired for future use.

3.0 Power, Transmission and Test Fixture

3.1 Power and Transmission

The cycloidal blade group requires in excess of 30 Hp to provide power and a suitable transmission to relay this power to the blade mechanism. Although the theoretical revolutions to obtain the thrust required is 650, the need exists to fine-tune the RPM to optimize the blade speed for maximum efficiency.

Increases in the power plant RPM changes the output power, so it would be advantageous to maintain the power at a known level and RPM, and alter the gear ratio. Conventional transmissions are not suitable for such fine adjustments and so a Continuously Variable Transmission (CVT) could be utilized to precisely alter output RPM. These transmissions are available through Honda and are electronically controlled belt-driven devices giving a gear spread in excess of 6:1. This allied to its least powerful engine (105 Hp) would provide a wide power and test band to determine the ideal revolutions for best propeller efficiency.

Various power trains were considered, discussed, and dismissed due to cost, availability, and particular suitability. While the Honda CVT transmission would suit this application well, it was far too

expensive and difficult to control due to the Phase I timeline. Transmissions in ATV machinery could not handle the torque and the horsepower was marginal. These transmissions are available in more substantial equipment and should perhaps be considered in future efforts to optimize blade speed control. For the Phase I test purposes, these systems have been deemed unnecessary.

The engine chosen for the Phase I testing was a stock Chevrolet 305 V8 mated to an automatic transmission. This may seem excessive, but we did not suffer from lack of power or torque while exploring the aerodynamic limits of the propeller. The engine transmits the drive to the propeller shaft through a Goodyear Eagle PD toothed drive belt incorporating a 1.6:1 reduction to enable engine RPM to be maintained. The overall gear reduction through this system is 5:1 therefore requiring 3,250 RPM to achieve a blade speed of 650. This system is capable of loads up to 70 Hp at 870 RPM. The power required was derived from a direct reading of the torque from the drive shaft.

3.2 Test Fixture

A significant requirement of this test was to ensure that the data collected from the propeller was in fact from the propulsion unit, rather than from any other external influence. RASPET team members aired concerns about the resonance of the blades being an unwelcome addition to the resonant frequency of the test fixture. The harmonics of the blades required 10-30 Hz oscillation.

The test fixture (Figure 6) is built using 3" 'C' section steel channel and heavy-duty pillow block bearings. The engine is mated to a suitable automatic transmission which is good for vibrations damping due to the mainly viscous fluid means of power transfer. The transmission is then mated to the final driveshaft via a Goodyear PD belt drive and reduction system, again absorbing vibration. The whole unit was tested to discover its resonant frequency, and results could not be determined because the Hz value was too high for the instruments to measure. This was very good news as it confirmed the solidity of the structure and ensured extremely smooth and vibration-free test runs.

Considerable emphasis was directed to the construction of the test fixture that would enable a cycloidal propeller to be run. The fixture was built to enable a wide range of RPM values from zero to 875, and angles of attack from zero to 45°. Such angles require more power and generate more torque than the predicted 28 horsepower and 230 foot pounds.

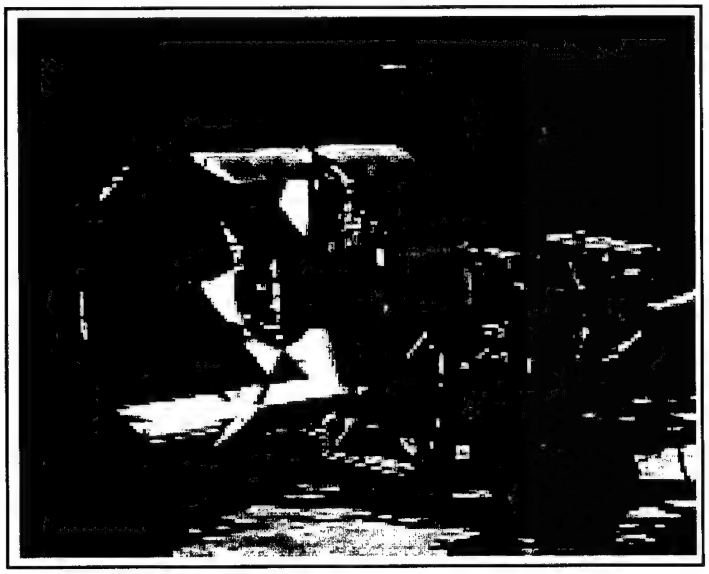

Figure 6. The cycloidal propeller on test fixture

In order to enable a 45° movement, the common link to all the blades must occur at 2.6 inches from the center instead of the 1.5 for the 26° AoA. The center mechanism is a graduated worm drive scale enabling off-axial movement from the drive shaft up to three (3) inches. This is a fixed system that, although relatively static, cannot be altered during a run.

4.0 AERODYNAMICS

From an aerodynamic standpoint, the larger the diameter of the blade group the better. Early experiments performed in the 1920's era showed mixed results, with some theoretical results being extremely promising only to be flawed by lack of true aerodynamic understanding and poor actual test data. However, over time test procedures have improved. Eastman obtained the most promising test results in 1945. He used large fifteen-foot (15') diameter multiple-blade wheels that ultimately displayed better performance than the theory suggests.

Rapid calculations by computers, understanding airflow, and of the forces generated by it have enabled the BOSCH Aerospace team to generate theoretical figures that show a more realistic picture. Our approach to analysis was based on, and developed from, finite-wing theory. The assessment is simplified by assessing the performance of a single wing rotating about a horizontal axis. Initial modeling results showed that lift generated by this system is significantly higher than that generated by other propulsion techniques available in conventional aircraft. To add realism, our research team modified the model by taking a generally conservative and more pessimistic approach. Nonetheless, the model showed that substantial improvements in lift versus horsepower were possible with the technique, and extremely promising numbers were generated. A promising correlation was found when comparing our modeling results with existing wind tunnel data (Eastman, 1945).

It was important to establish the best angle of attack for the blades rotating at the correct revolutions per minute. As can be seen in the plots in the RASPET report (provided as Appendix A), power required and the thrust generated by it, have changed little from the first computer printouts, but the detail and our understanding have improved considerably. One notable addition to the lift, drag, and lift loads is the appearance of a side load. This was not initially expected, and along with the asymmetrical lift and loading plots, can also be seen in Appendix A.

Some aspects of the aerodynamic modeling could not be determined however in the time available, i.e. airflow issues, specifically inner-blade airflow and downwash. The blades in rotation follow closely behind each another and experience the wake from the proceeding one; consequently the blade angles of attack are higher than would normally be expected from a standard wing to generate maximum lift. Figure 7 depicts a standard wing at relatively low AoA in early stages of stall. The downwash issue is of similar origin. Airflow from the top blade is directed downward into the path of the opposing blade which is now experiencing incoming air at a higher angle of attack than if clean air. It would therefore be beneficial for the bottom blade to have a larger angle of attack than the top one to compensate.

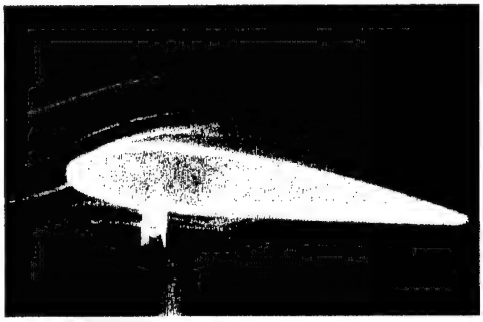

Figure 7. Standard wing at low AoA

Due to the nature of the Phase I effort and the need to impose limiting factors in the physical design, initial computations were based on a blade configuration constrained to a four-foot diameter. Without such limitations the rotational diameter of the cycloid would be infinite as the computer determined optimum lift. Previous studies, such as the Eastman report, showed that the ideal blade length matched the rotational diameter. These findings were enhanced by Kurt Kirsten who wrote,

"The best proportions would naturally be a blade length equal to the orbit diameter, thus providing for maximum slipstream area with minimum dead air envelope." Application of this theory to the computer model resulted in verification. Thus, our choice of a four-foot diameter disk was fitted with a four-foot blade length.

The number of blades that can be incorporated into the design should be as high as aerodynamically possible to maximize active blade 'air time.' This was mentioned by Kirsten, and was later shown in computer modeling that with four or more blades, the system became more stable and less erratic.

It can be shown that with one blade, there is a very large oscillation in both the centrifugal loads and aerodynamic loads. With two blades, the centrifugal loads are balanced, but the aerodynamic loads still produce significant oscillations. With three blades, the aerodynamic loads become fairly smooth, but the centrifugal loads are not balanced. With four blades, both the centrifugal and the aerodynamic loads become smooth with only very small oscillations. An example of this is a four-bladed helicopter, which are smoother and quieter than the two-bladed types.

Therefore, for our purposes, six blades were considered to be the minimum required to produce smooth and continuous thrust and the maximum without excessive turbulence and inter-blade flow interference. Appendix I shows the computational results of a six NACA 0012 bladed cycloidal system of diameter four feet. Each blade being four feet long and having a 4:1 aspect ratio. The blades are rotated at 650 RPM at an angle of attack of 25° and require a little over 28 Hp to generate 350 pounds of thrust (i.e. 12.5 pounds of lift for each Hp). It should be noted that while these power requirements look very good, they are based on aerodynamic issues only. Additional power was expected to be required to overcome friction and other forms of energy transfer loss and so thrust/ Hp could be reduced to eleven (11).

Further improvements and refinements were made to the modeling addressing the unsteady aerodynamics question. These additions were important in determining the AoA required obtaining optimum lift. It should be noted that a NACA 0012 section would normally stall at 16° (Figure 8).

Because of the complex issues of airflow interaction between the blades, the mechanics of the test fixture enabled an infinite ability to adjust the AoA from between zero and 45°.

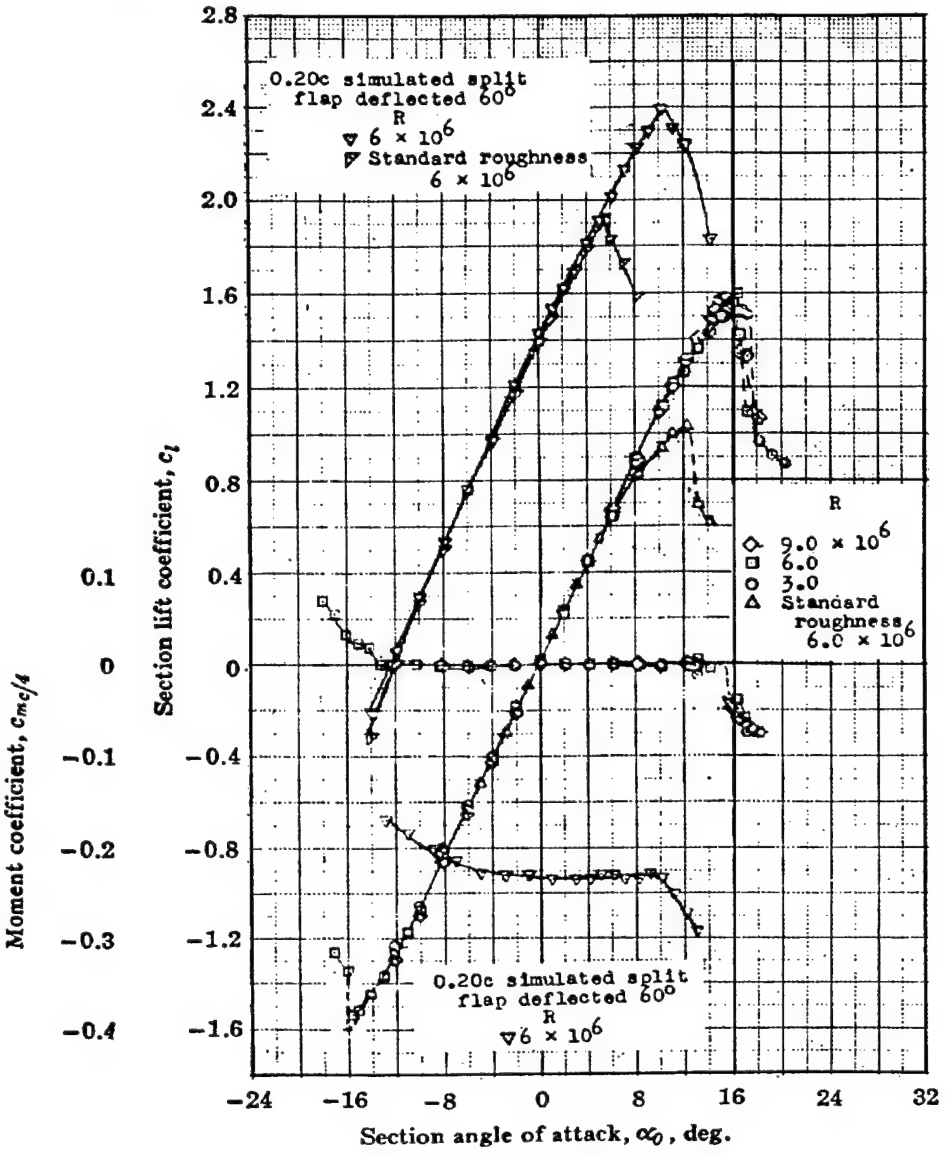

Figure 8. Graph illustrating the lift coefficient against AoA. maximum CL obtained at 16°

5.0 TESTING

During October 1998, the first Cycloidal Propeller intended for flight since 1946 was run and tested by the BOSCH Aerospace team at a facility in Huntsville, Alabama. It was then moved to the RASPET facilities for thrust tests, and to prepare for the Government demonstration on November 9th.

Based on the computations and experimentation of one of the most successful ground tests of this century, the Wheatley runs of 1935 utilizing a fifteen-foot diameter blade group promised impressive thrust figures. The RASPET computer model showed similar thrust figures using a diameter of only four feet. The expected thrust of 350 pounds could be achieved at 650 RPM with blade AoA set at 25°. Modern computer technologies could not, however, determine accurate flow between the blades of a

cycloidal unit, nor provide a clear understanding of the resultant downwash in the time allocated. Consequently, the test fixture enabled AoA of up to 45° and power reserves in excess of the estimated 28 Hp to accommodate unforeseen test requirements. Initial runs did not involve the blades or any of the control rods to determine hub and blade arm balance and stability. Chadwick Helmuth 8500 series apparatus recorded the motion of the system via specifically located accelerometers (Figure 9). These runs, conducted at Huntsville, incorporated the dynamic balancing of the system to ensure the true running characteristics of the test fixture before the aerodynamic tests commenced. This procedure involved the incremental increase in engine RPM from zero to 3,000 (0-600 at the output shaft). The recordings concluded that the test fixture required no further improvement to the balance, and blade control components could be added to start the thrust tests.

Figure 9. Motion Testing

Upon running the system with blades and control mechanisms, the propeller was run initially at a slow speed. Although it was surprising how quietly the Chevrolet engine ran after being removed from the donor vehicle, it was even more encouraging that it was the dominant source of noise when the cycloidal unit was engaged. The RPM was tentatively increased to a blade speed of 250 RPM and still, it was barely audible except for a curious regular tapping noise. (This noise was later identified and resolved.) Satisfied with the integrity of the system, the test fixture then proceeded to the RASPET facilities for thrust tests.

The test fixture was located on a three-point mounting, the single rear pivot point being fixed to provide a moment arm, while the two forward feet were housed on the Evergreen Road Runner 5,000 pound aircraft load cells for thrust measurement (Figure 10). A third 2,000-pound load cell would be required to measure the torque generated by the blade group and consequently, knowing shaft RPM, the horsepower needed to drive the blades. This number could also be estimated by the aerodynamics engineers, but would be less precise due to 'real world' anomalies.

The two forward load cells were mounted as far apart as possible to provide not only greater stability to the system but to enable a more accurate measurement of the aerodynamic torque generated by the blades. The whole rig could then be adjusted to be horizontal with a digital level, ensuring accurate readings.

At the RASPET facility, the propeller was located outside the hanger with the engine section of the test fixture inside. Closing the hangar doors on each side of the test fixture provided protection to the operating crew should any type of failure occur. An optical tachometer determined output shaft RPM to within one revolution, and gave the engine operator a clear digital reading. All three load cells could be read from their control box inside the building, either individually or in combination with either of the other two. Two Hi-8 video cameras were set up on tripods to record events prior to a systems check before the first load test of the blades. A fire-up sequence checklist involved the usual inspection of the blade group, drive system, safety systems and the power plant.

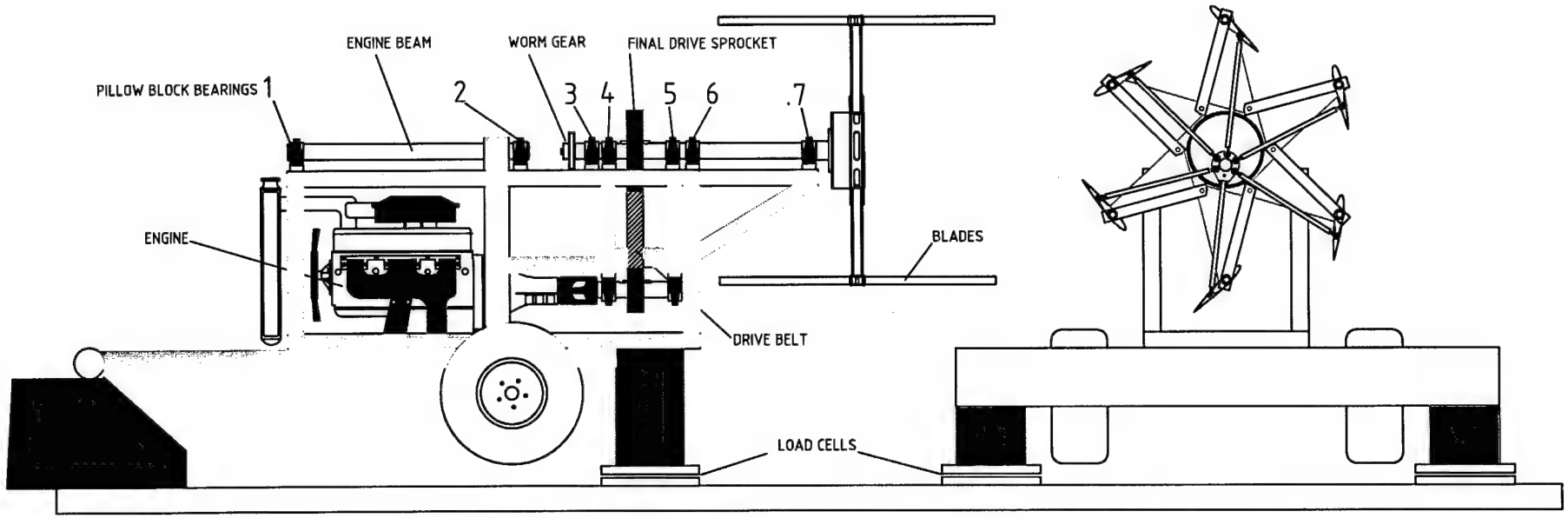

Figure 10 Cycloidal Test Fixture

The first load tests were conducted at 15° AoA with the RPM steadily increased to 350, but then shut down because the regular tapping sound was back. Concerned that this noise could be causing damage that could result in a high-speed failure, the rig was shut down to determine the cause. After the 0.1mm shim had been inserted in the thrust angle adjustment-retaining block next to the systems operator, tests could continue. After the AoA was increased to 25° the revolutions were increased to 550 to check the high-speed running of the structure before the real load tests could commence. This high-speed run uncovered one critical manufacturing failure in the Master Control Rod welding. This failure caused an uneventful halt to proceedings and another master rod required fabrication. During these high-speed runs it was noted that the blades were developing a few degrees of dihedral, probably due to the spar not running the whole length of the wing. This initially was of little concern, but did limit our speed to below 450 RPM in order not to induce failures in the blades themselves.

With the master rod repaired and other minor irritations resolved, test runs started at 25° which was the theoretical maximum angle that the blades could generate efficient vertical thrust. Several measurements were recorded up to 450 RPM, at each increment the thrust vector angle was adjusted each side of TDC to determine where maximum thrust was occurring. As the RASPET figures had predicted, lift fell off if the angle went past TDC and reached its maximum at 17° before TDC (BTDC) (Figure 11, page 16). At 25° AoA however, the lift numbers were fairly modest, recording 92.4 pounds of thrust. We increased RPM to 500 and recorded a maximum of 153.23 pounds of lift. The thrust values were below predictions. Thus, the blade angle was increased to 30°. This higher AoA requirement was expected since the inter-blade flow relationships could not be easily modeled, thus a greater range of angle adjustment was built into the test fixture.

At 30° AoA, the lift figures were much better and paralleled the ideal thrust curve, but at a level consistently 20-30% below it. We believe that the explanation lies in the missing polycarbonate air shield that was to cover the gap between the blade halves. Higher aspect ratio wings generally improve efficiency. The test blades had a theoretical aspect ratio of 4 (4 foot span and 1 foot chord), however, the gap between the blade halves (due to the missing polycarbonate plates) caused the wings to act as two independent lift devices with aspect ratios of 2. Additionally, the gap between the blade halves was a source of significant turbulence, especially as RPM increased. Thus, blade efficiency was reduced by as much as 30%. During the Phase I Option period, we hope to repair and install the polycarbonate plates, and reassess lift performance.

Ground effect and its most helpful properties are sometimes welcome in aircraft, but in this application it proved to be a minor disadvantage. With the blade group so close to the ground, air was being deflected back into the blades and disturbing flow around the bottom blades. We took this opportunity to investigate the airflow properties of the blades.

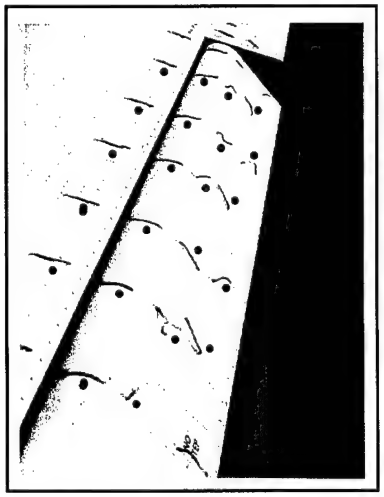

Figure 12. Airflow

To better understand the aerodynamics of the blades and to determine where and how flow separation was occurring (ref: Figure 7, page 11), small tufts of wool were attached to the subject airfoil surface prior to airflow testing. The photograph in Figure 12 shows smooth airflow where the tufts are marked in blue. The red tufts are clearly in disturbed air where airflow separation is occurring.

1	Maximum Vertical lift at 17° BTDC
2	Maximum Down Thrust at 163°
3	Shows Control Carriage at 45°

Figure 11

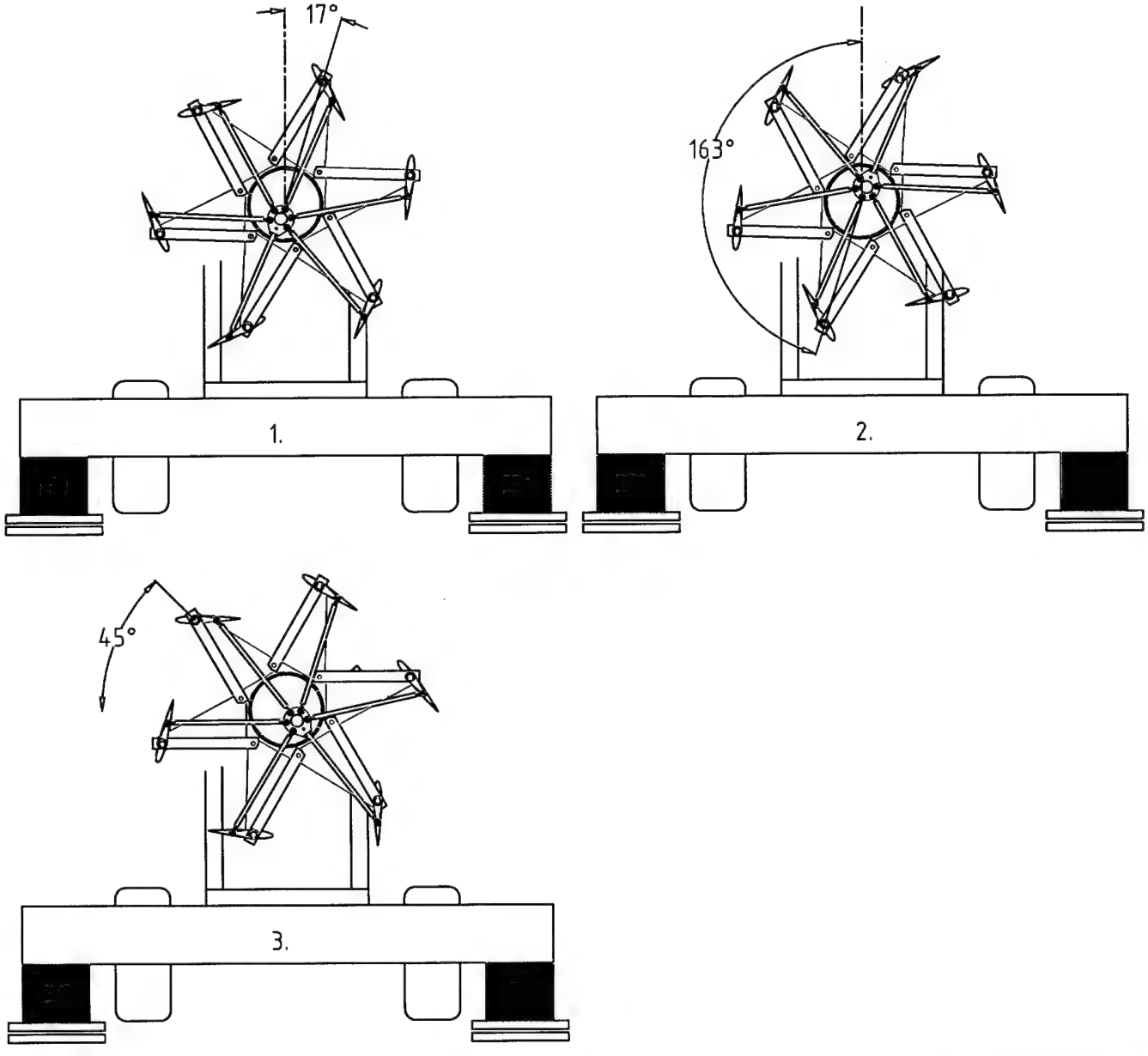

Airflow testing was conducted on a pair of the cycloidal blades. Using a strobe light to isolate the blades in rotation and to illuminate the tufts, the system was tested at 25°, 30° and 29°. In order to film the results, the thrust was vectored so that the active blades, at maximum AoA could be seen by the camera.

A sequence of four pictures is provided as Figure 13. *Figure 13.a* shows the tufts being attached to the blade; *Figure 13.b* shows the results of runs at 25° where the flow is smooth; *Figure 13.c* shows the results of runs at 30° where the blade is showing signs of stalling; and *Figure 13.d* shows the results of runs at 29° where maximum angle of attack could be achieved without compromising the blade efficiency. All were taken at the same RPM.

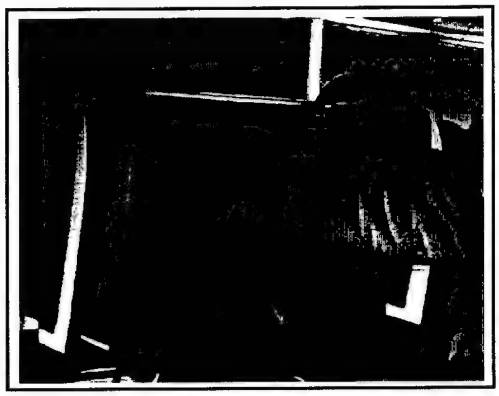

Figure 13.a Tufts being attached to blade

Figure 13.c Blades at 30° AoA showing signs of stall. The tufts can clearly be seen to be disrupted.

Figure 13.b Blade at 25° AoA

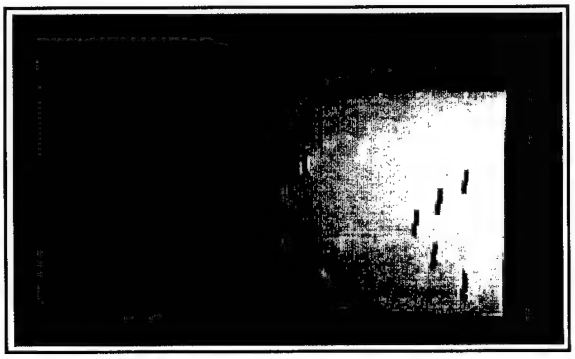

Figure 13.d A fine adjustment back down to 29° AoA and the tufts are back to clean airflow.

In addition to the "tufts test," a smoke machine gave us a good visual impression of how the air was moving throughout the blade system (Figure 14.a). Altering the thrust angle to 45° showed us how effective the cycloidal propeller is at directing flow (Figure 14.b).

Figure 14.a Vertical Thrust Down

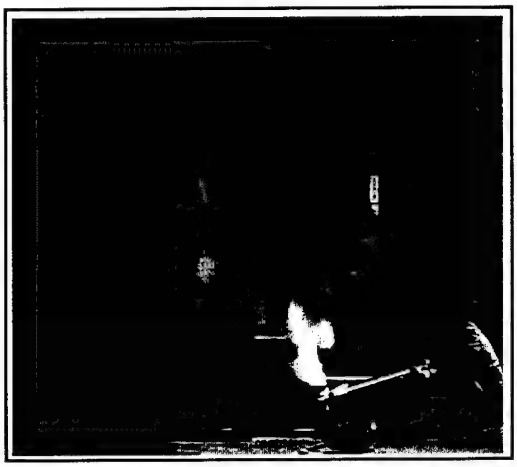

Figure 14.a Thrust Vector at 45°

The flow of air through the cycloidal propeller was found to be highly structured. The flow is constrained to a very narrow sector, and highly directional. Very little loss was observed over the blade ends. Although the testing was conducted with a known deficiency (the lack of polycarbonate covers over the gap between blades), the vector capability remained highly directional throughout the 360° arc. We believe that substantial improvement in overall thrust and in flow structure is possible once the gap covers are installed.

The graphical representation provided at Figure 15 shows the theoretical computer model developing 10.57 pounds of thrust per horsepower. Test data is displayed for "in ground effect" and "out of ground effect" test runs. A best curve fit projects output at higher RPM. The green "out of ground effect" plot is particularly interesting because of projected high level of performance. Reading from these data, we can say that the maximum thrust available within experimental error parameters is between 8.4 and 10.88 *lb/Hp*. If we are able to regain aerodynamic losses (30%), the system could achieve thrust levels between 14.14 and 10.92 *lb/Hp*.

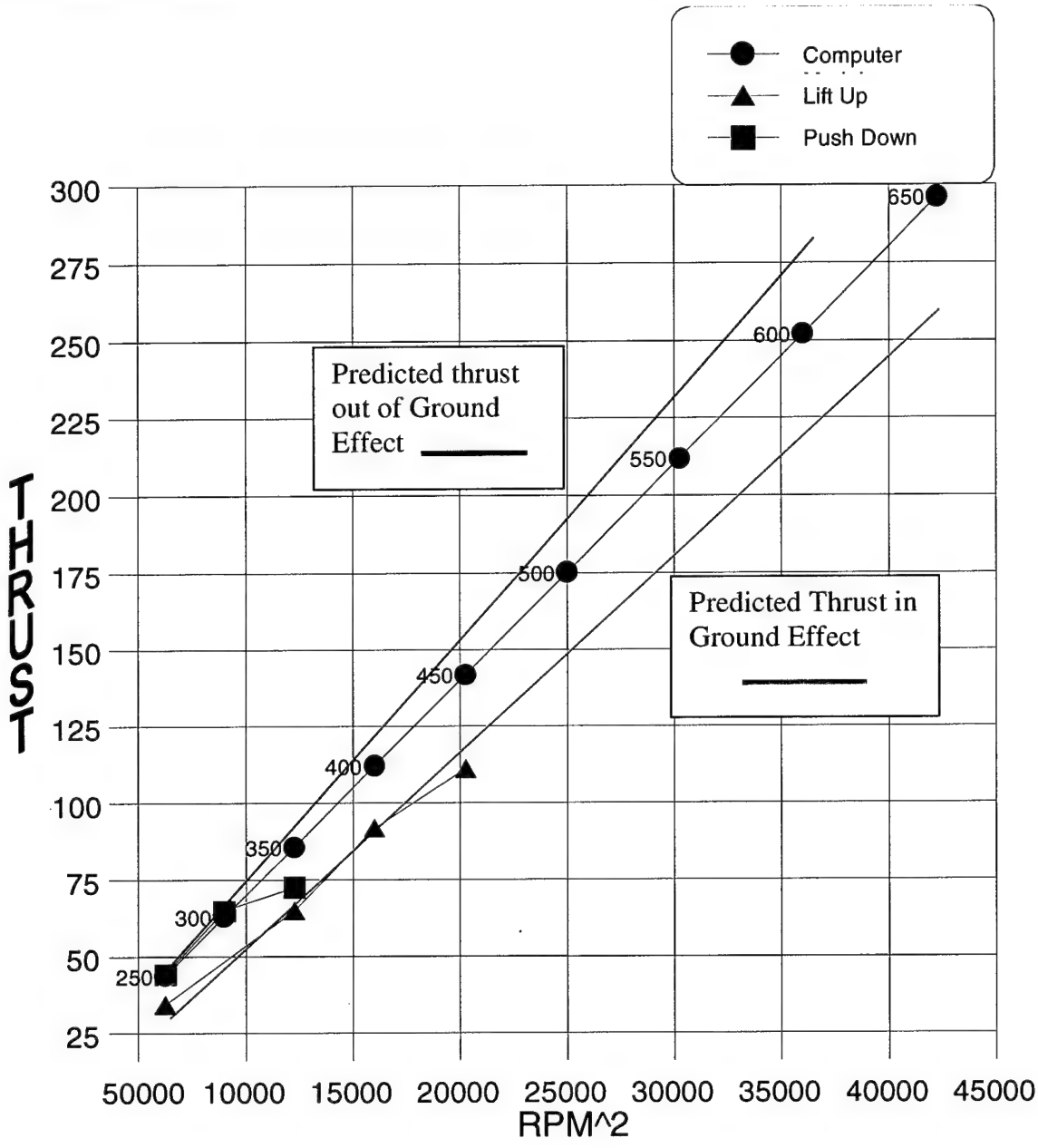

Figure 15. Theoretical Computer Model

The plots show only one inconsistent data point; in the "out of ground effect" data. We believe that this is due to a bad reading and have discounted the data point. Additional testing will be conducted in the option period to further validate out of ground effect thrust performance. Our worst case thrust figures, even with mid-blade airflow disruption, are competitive with the world's best helicopter systems.

APPENDIX A
RASPET REPORT

Final Report on Cyclic Propulsion Computer Modeling

Michael McNabb

APPENDIX A

Dr.George Bennett
Mississippi State University
RASPET Flight Research Laboratory
Department of Aerospace Engineering
Mississippi State, MS 39762

Background

Reasons why we chose this configuration.

The final configuration was a system of six blades, evenly spaced around a 4 ft diameter orbit. The blades were NACA 0012 airfoils with a 4 ft span and a 1 ft chord. To get the 350 pounds of lift specified for the system, the mechanism needed to rotate at 650 RPM.

Six NACA 0012 blades with constant chord
Diameter of the orbit = 4 ft.
Span of the blades = 4 ft.
Chord of the blades = 1 ft.
Speed of rotation = 650 RPM

Airfoil

The NACA 0012 airfoil was chosen because it is a standard symmetric airfoil with good lift.

Diameter

In general the larger the diameter of the orbit, the better it is. With this in mind, the diameter was set at 4 ft because that was as large as we thought we could fit on the proposed VTOL UAV to be made in stage three of the proposal.

Span

The span of the blade was set at 4 ft. In the report 'Cycloidal Propulsion Applied to Aircraft' by Fredric Kurt Kirsten, he stated "The best proportions would naturally be a blade length equal to the orbit diameter, thus providing for maximum slipstream area with minimum dead air envelope."

Number of Blades

It was mentioned by Kirsten and later shown in computer modeling that with four or more blades, the system became more stable and less jerky. For example, a four bladed helicopter is smoother and quieter than the two bladed Huey. With this in mind we decided on a six blades system.

Chord

In general the further apart the wings are the better they perform. This is hard to do in a 4 ft diameter orbit. The chord was set at 1 ft because this

allows one chord length between blades for free airflow. In other words, half the circumference of the orbit is blade, and half the circumference of the orbit is free air.

Speed of Rotation

In general the slower the system turns the better, but you still have to generate the required 'q', or dynamic air pressure, over the blades. To get the 350 lbs of lift from the system, it needed to rotate at 650 RPM.

Program Development

Ideal sine motion with steady aerodynamics

The basis for the motion of the blades in the computer modeling is a sine-cosine wave. At top-dead center (TDC) the blade is at a maximum angle of attack (AoA) or maximum alpha. At bottom-dead center (BDC) the blade is at a minimum AoA. At the horizontal position, the AoA is zero.

Equation 1.

$$\alpha = \alpha_{max} * \sin(\theta)$$

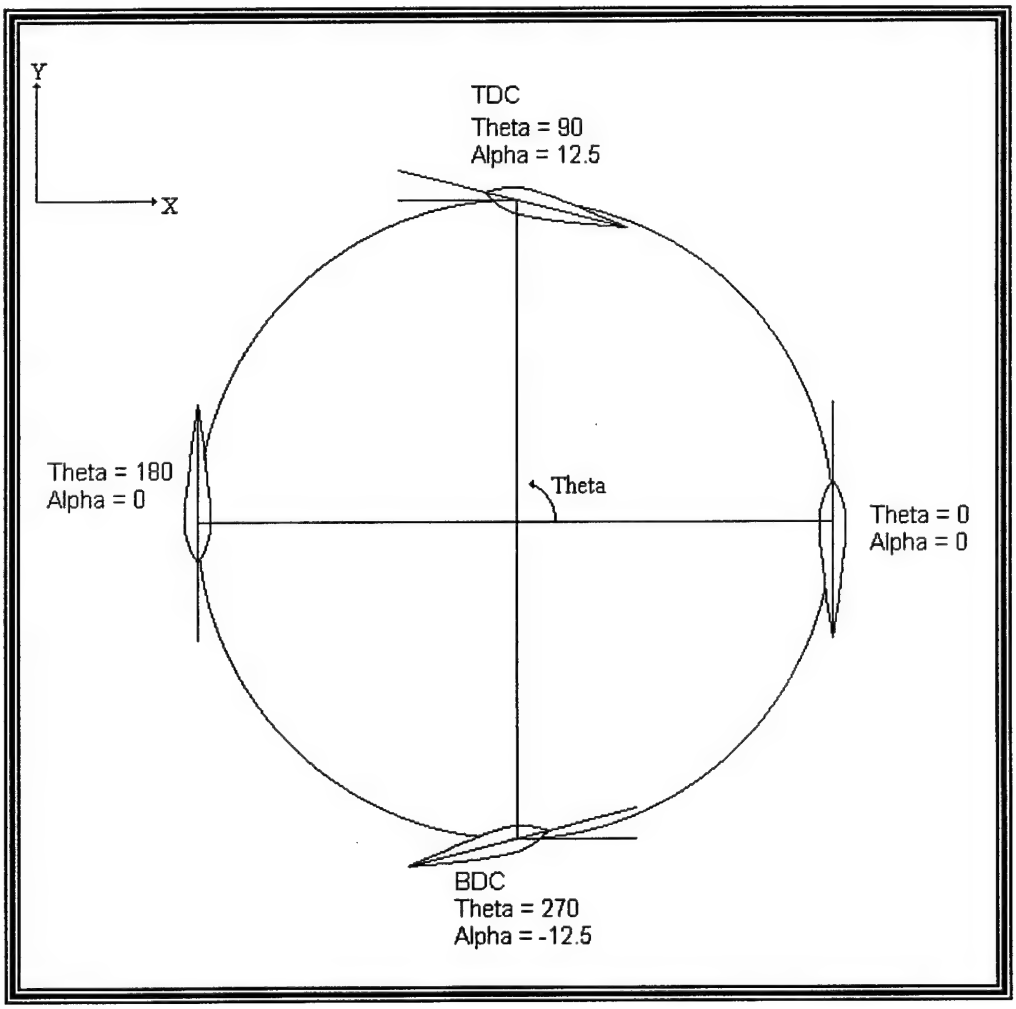

Using steady aerodynamics, the lift and drag of the blade can be determined for the following equations.

Equations 2, 3, 4 and 5.

$$C_L = C_{L\alpha} * \alpha$$

$$C_D = C_{D0} + \frac{C_L^2}{\pi * AR * Eff}$$

$$Lift = \frac{1}{2} * \rho * Vel^2 * S * C_L$$

$$Drag = \frac{1}{2} * \rho * Vel^2 * S * C_D$$

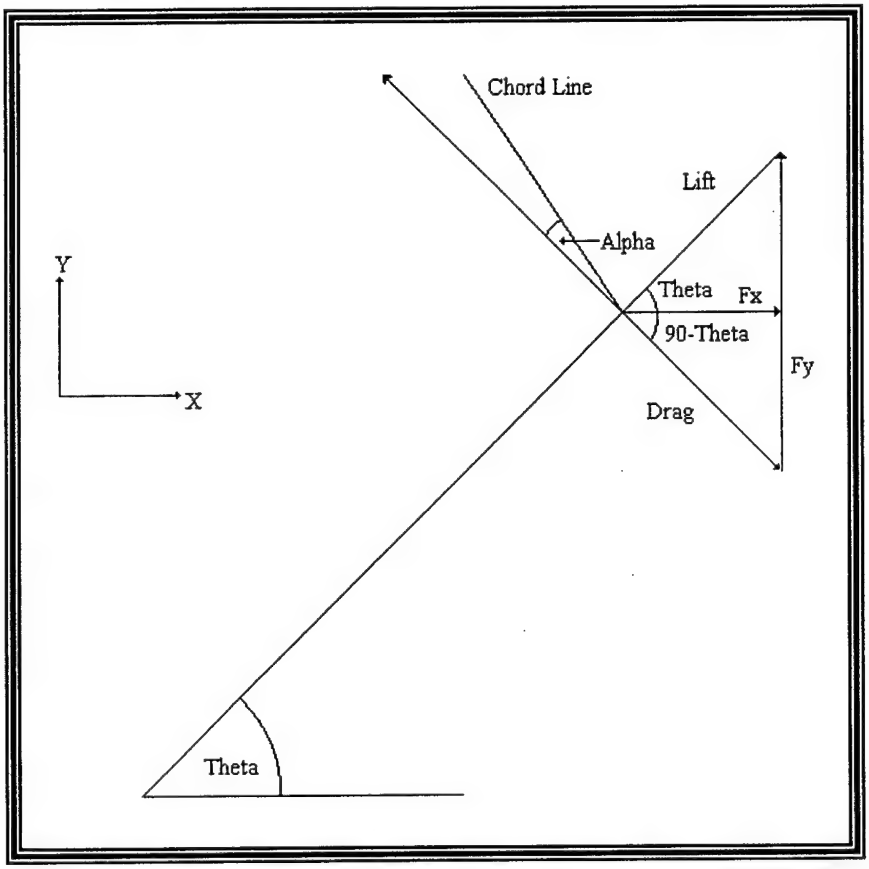

The total lift or thrust of the mechanism is the sum of all the lifts produced by the blades.

Equation 6.

$$Lift_{mechanism} = Fy = \sum_{i=1}^{Number\_of\_blades} \{Lift_i * \sin(\theta_i) - Drag_i * \sin(90 - \theta_i)\}$$

The power required to turn the mechanism, is the sum of all the drags produced by the blades times the velocity that blade sees. The '550' is to convert to horsepower.

Equation 7.

$$Power_{required} = \sum_{i=1}^{Number\_of\_blades} \frac{Drag_i * Vel}{550}$$

The program was designed to iterate to the required lift (350 lb.) by increasing or decreasing the maximum AoA.

Two-dimensional aerodynamics is based on infinite airfoil tests, where the air does not feel the disturbing effects of the wing tips, the tip vortex. Using two dimensional steady aerodynamics, the maximum AoA needed was 12.6°.

Three dimensional aerodynamics is an adjustment of two dimensional aerodynamics. This adjustment allows the air to feel the effects of the wingtips. Using three-dimensional steady aerodynamics, the maximum AoA needed is 20.0°.

This is a large change is caused by the wing tip vortex. Because the blades are comparatively short, most of the blade can feel this wing tip vortex. This effectively makes the blade seem like it is at a lower AoA than it really is. This reduces the lift the blade can make.

Real motion with steady aerodynamics

The mechanism is a collection of four bar linkages that control the AoA of the blades. By moving one of the joints common to all the linkages (Point O4 in the following figure) the maximum AoA of the blades can be changed. This distance is called the offset.

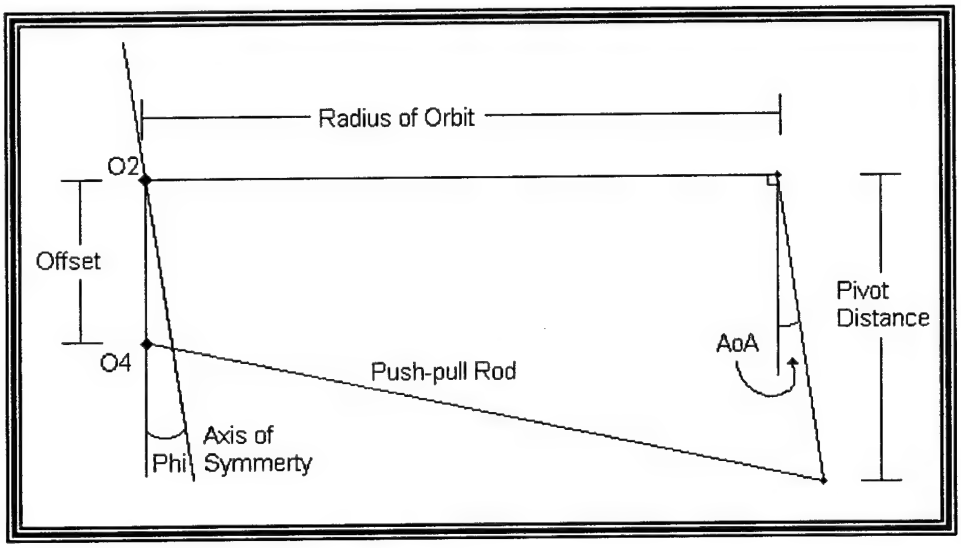

The AoA of the blades as they go around the orbit is determined by using the procedures laid out in the textbook Mechanics of Machinery. This textbook derived a series of equations based on the geometry of the four bar linkage (the length of the bars).

The motion of the mechanism will, unfortunately, not be a pure sine-cosine wave. It is close, but not perfect. This pseudo sine-cosine wave is shifted about 5 degrees. In other word the maximum AoA does not happen at TDC, but at 5° after TDC. Because of this a force is produced perpendicular to the desired lift/thrust. This side force must be balanced by rotating the axis of symmetry. The amount the axis of symmetry is rotated is called ϕ.

Using steady aerodynamics and the data in the background section, the offset needed was 0.855 inches, with a ϕ of -6.14° (in the opposite direction the mechanism is turning). The offset gave the max AoA required for steady aerodynamics (20.0°).

Ideal motion with unsteady aerodynamics

In this program we used the ideal sine motion with the unsteady aerodynamic equations for the lift and pitching moment of the blade as it went around the orbit. The reason we need to use unsteady aerodynamics is, it take a finite amount of time to develop lift. Steady aerodynamics does not take this into account. The blades are moving and rotating fast enough to make steady aerodynamics a bad assumption.

The unsteady lift and pitching moment equations requires the angular velocity and angular accelerations of the blade. To get this the angle of attack equation was differentiated with respect to time.

Equation 8, 9, and 10

$$\alpha_{blade} = \alpha_{\max} * \sin(\theta) = \alpha_{\max} * \sin(\omega_{system} * t)$$

$$\omega_{blade} = \alpha_{\max} * \omega_{system} * \cos(\omega_{system} * t)$$

$$Acc_{blade} = -\alpha_{\max} * \omega_{system}^2 * \sin(\omega_{system} * t)$$

With this information the unsteady lift, drag, and pitching moment can be calculated for the blade. With the lift and drag produced by each blade, the total lift/thrust force the system can produce, and the power required to turn the mechanism can be calculated. Using the pitching moment, the needed push rod force can be calculated.

Using the data in the section called background, the following was calculated. To produce 350 lbs of lift/thrust, you need a maximum AoA of 25.36°, and a ϕ of 27.87° (in the direction of motion).

Real motion with unsteady aerodynamics

In this, the final version of the computer modeling, the true motion due to the mechanism, and the unsteady lift equations were combined. This program should model everything but the interaction between the blades. We are still working on a good way to model this interaction.

Using the data listed in the section entitled background, the offset needed is 1.075 inches, and a ϕ of 21.62° (in the direction of motion). This ϕ of 21.62° is the 27.87° caused by unsteady aerodynamics and the –6.14° caused by the mechanism itself. The data from the program that combined the real motion and the unsteady aerodynamics, is plotted in the appendix 1.

Analysis of the Real Motion with Unsteady Aerodynamics

Explanation of Appendix 1.

Plots 1, 2, and 3.

The first three plots show the angle of attack, angular velocity, and angular acceleration. The angle of attack is a close match to an ideal sine wave. The angular velocity and acceleration show that higher harmonics are present, because they are increasingly unsymmetrical.

Plots 4, 5, and 6.

In the plots of lift, drag and pitching moment per blade, it can be seen that the peaks do no occur at the regular places (0°, 45°, 90°,...). This phase shift is caused by the mechanism, and by unsteady aerodynamics. In other word it does not follow nice simple equations like equations 8, 9, and 10.

Plots 7, and 8

These plots show the component of lift from a blade in the direction the mechanism is lifting or thrusting and the side forces produced.

Plot 9

Plot 9 shows the forces the push rod will need to withstand. It says that the rod must hold 200 lbs of compression. It also needs to hold more than that for fatigue reasons.

Plots 10, and 11

These plots show the power and torque needed just to turn the mechanism. This does not count the power feed to the push rods or other power hungry systems. Also notice that there is some variation in the power and torque requirements. This thing will want to shake.

Plot 12

Plot 12 shows the lift/thrust the system can produce. In this plot you can see the variation in the lift/thrust force. Again the mechanism will shake.

Analysis of all Four Program Models

Explanation of Appendix 2.

The four computer models were;

1. Ideal sine motion with steady aerodynamics
2. Ideal motion with unsteady aerodynamics
3. Real motion with steady aerodynamics
4. Real motion with unsteady aerodynamics

These four models are compared in the following plots.

Plot 13

Plot 13 shows the lift per blade as the blade goes around the orbit. They all look roughly the same magnitude because each of the four programs iterated to the required 350 lbs. of lift or thrust. Mechanism and the use of unsteady aerodynamics caused the phase shifts.

Plot 14

This plot shows how the AoA must be increased each time we go to a more complex aerodynamic model (from the sine motion with 2D aerodynamics to the real motion with unsteady aerodynamics). This is because the more complex aerodynamic models account for more things than the simple ones.

Plots 15 and 16

These plots show how the higher harmonics of the more complex motions start to show up. Notice how the curves become more unsymmetrical with the inclusion of unsteady aerodynamics.

Plot 17

Plot 17 shows the drag per blade as the blade goes around the orbit. Notice that the drag peaks at the same time as that models lift peaks.

Plot 18 and 19

Plot 18 shows the lift or thrust produced by a blade in the direction the mechanism is lifting or thrusting. Plot 19 shows the side forces produced by a blade as it goes around the orbit.

Plot 20 and 21

These plots show the torque and power required to turn the mechanism. Notice that the torque and power increases as the computer model get more complex. Also notice that the unsteady analysis shows some oscillation in the torque and power.

Plot 22

Plot 22 shows that the average lift or thrust produced by the system is about 350 lbs.

Appendix 1.

Plots of the Behavior of the Real Motion with Unsteady Aerodynamics

Six NACA 0012 Blades
650 RPM
Radius = 2 ft
Pivot Distance = 2.5 inches
8 lbs/Blade
Span = 4 ft
Chord = 1 ft
Offset = 1.03 inches
Phi = -32.78
Plot 1.

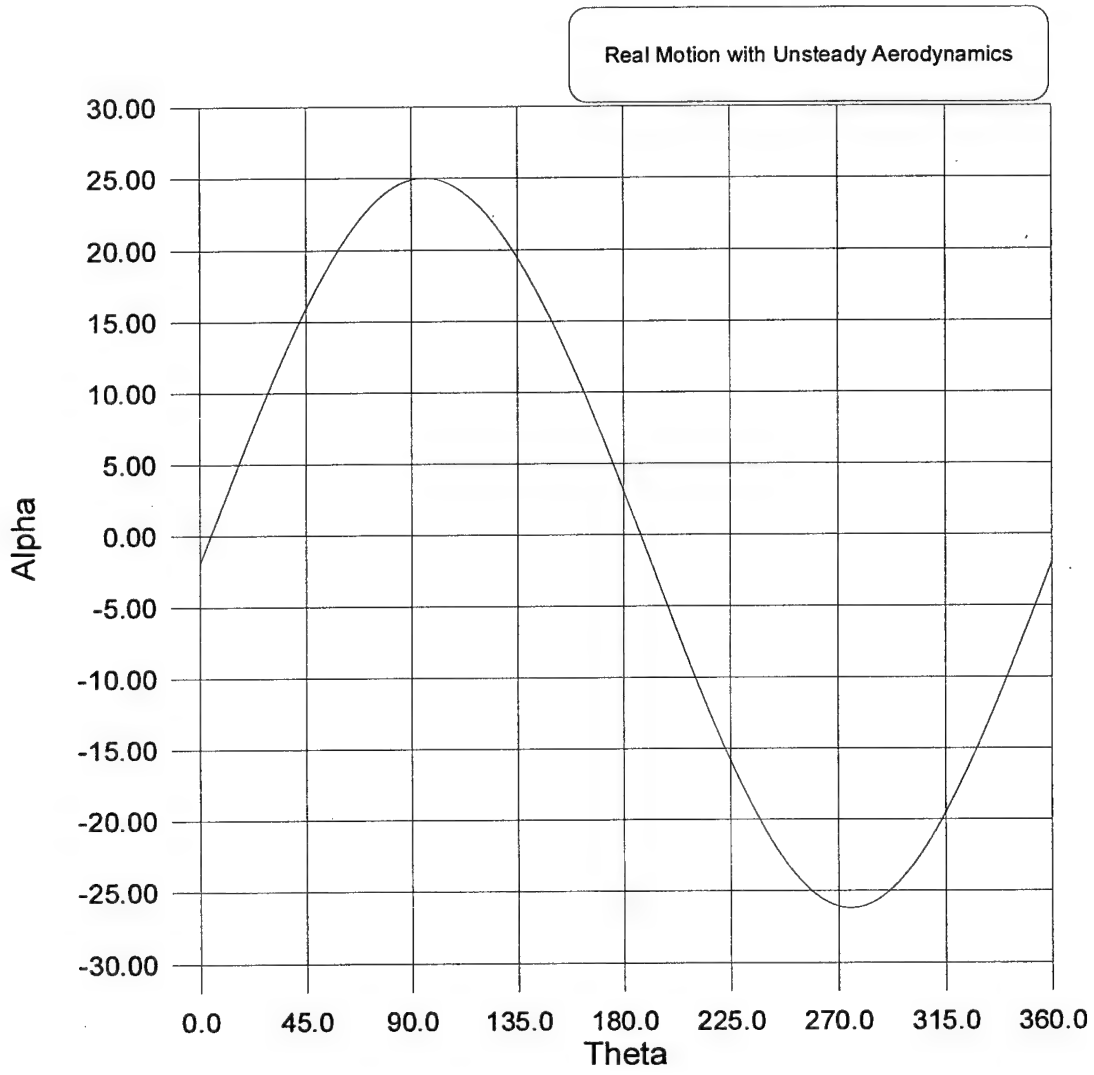

Six NACA 0012 Blades
650 RPM
Radius = 2 ft
Pivot Distance = 2.5 inches
8 lbs/Blade
Span = 4 ft
Chord = 1 ft
Offset = 1.03 inches
Phi = -32.78
Plot 2.

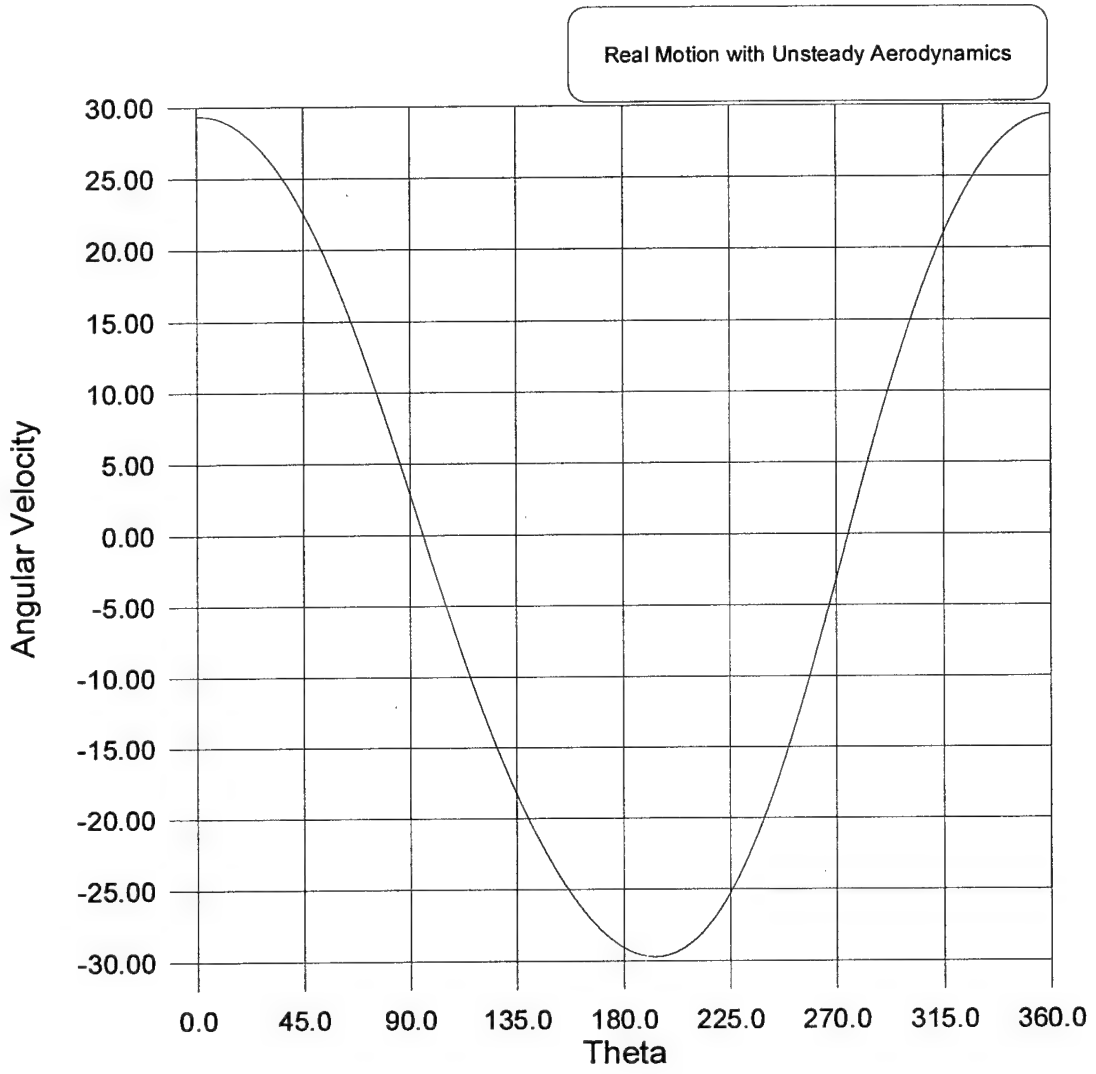

Six NACA 0012 Blades
650 RPM
Radius = 2 ft
Pivot Distance = 2.5 inches
8 lbs/Blade
Span = 4 ft
Chord = 1 ft
Offset = 1.03 inches
Phi = -32.78
Plot 3.

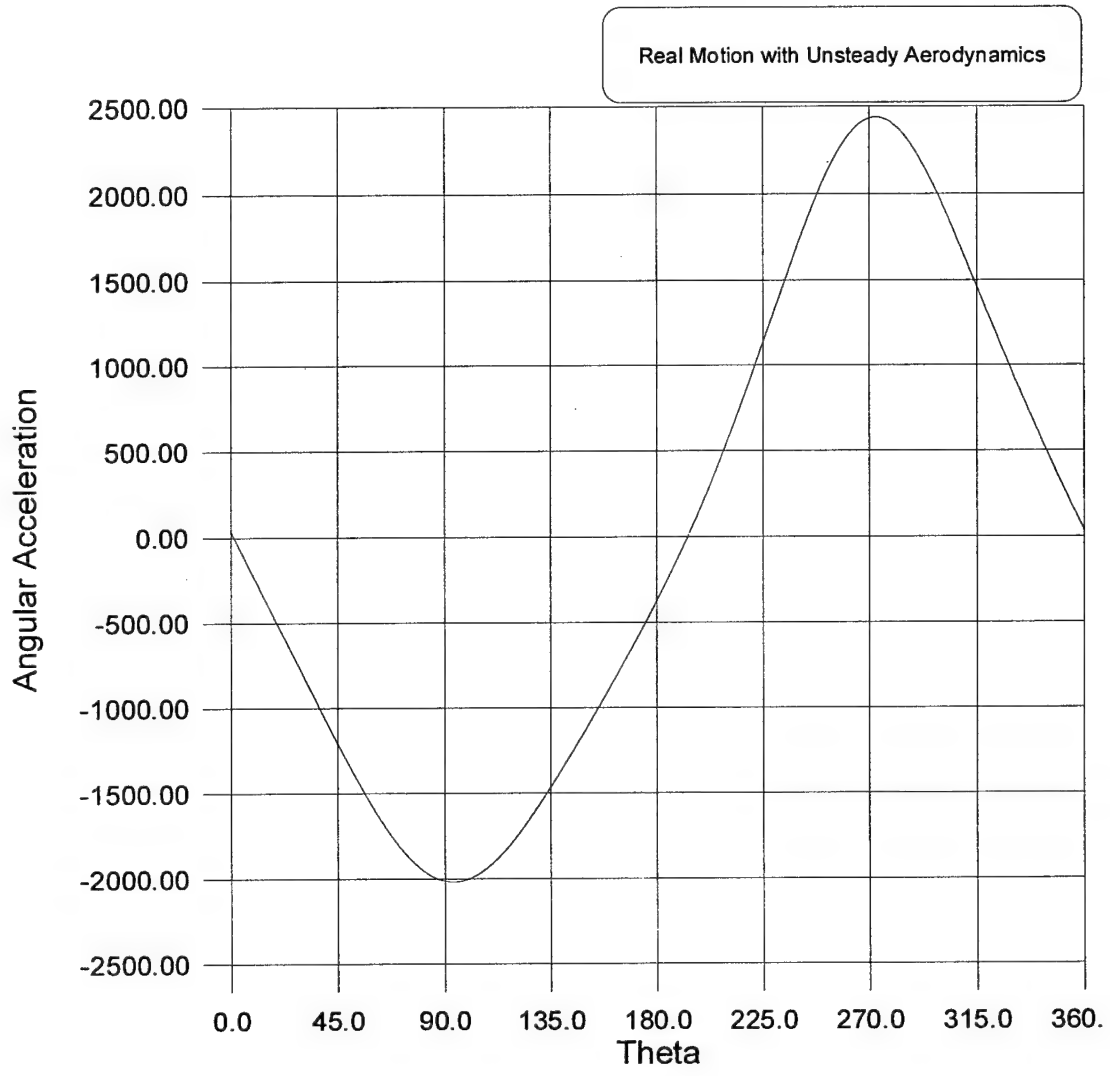

Six NACA 0012 Blades
650 RPM
Radius = 2 ft
Pivot Distance = 2.5 inches
8 lbs/Blade
Span = 4 ft
Chord = 1 ft
Offset = 1.03 inches
Phi = -32.78
Plot 4.

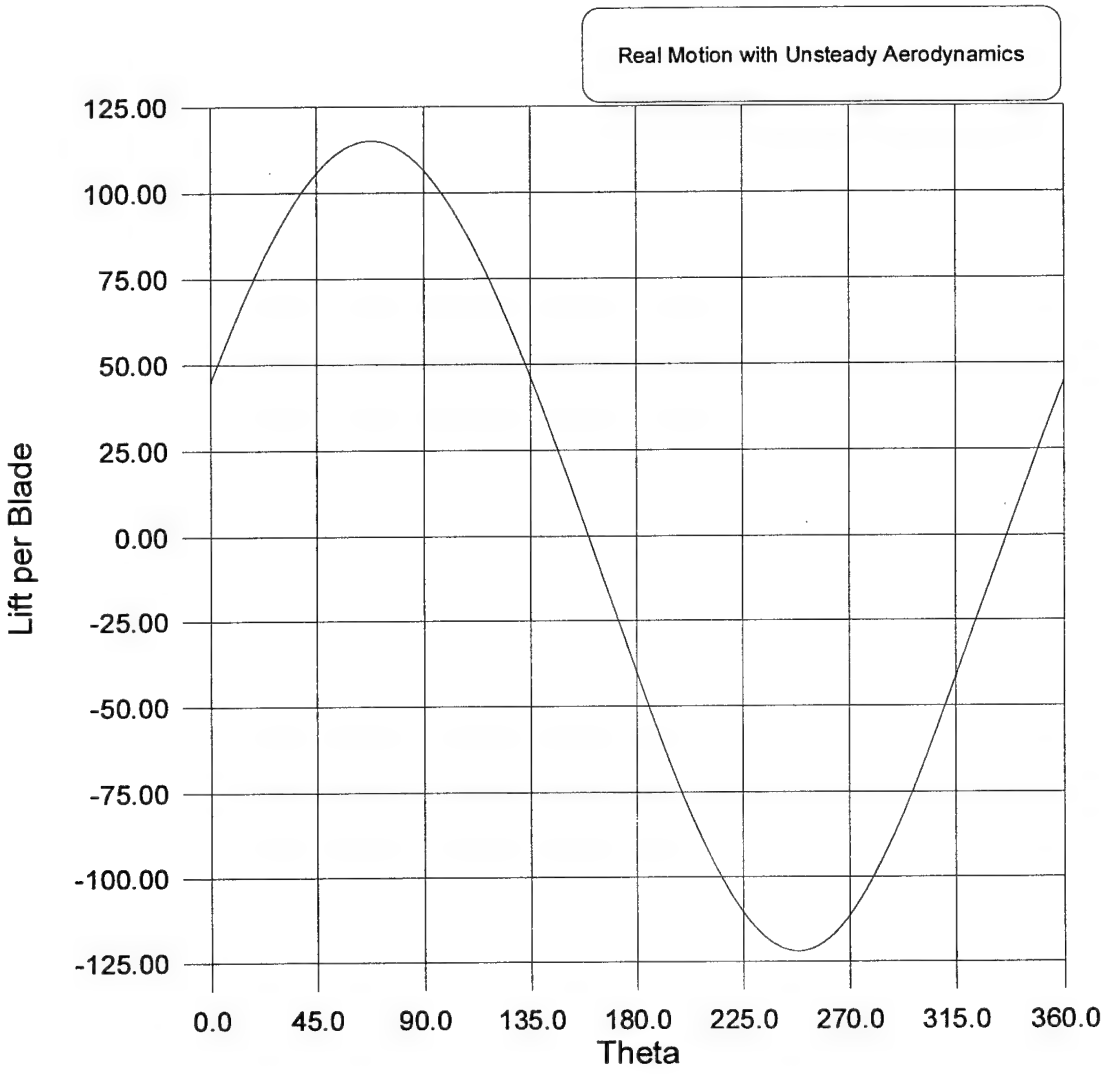

Six NACA 0012 Blades
650 RPM
Radius = 2 ft
Pivot Distance = 2.5 inches
8 lbs/Blade
Span = 4 ft
Chord = 1 ft
Offset = 1.03 inches
Phi = -32.78
Plot 5.

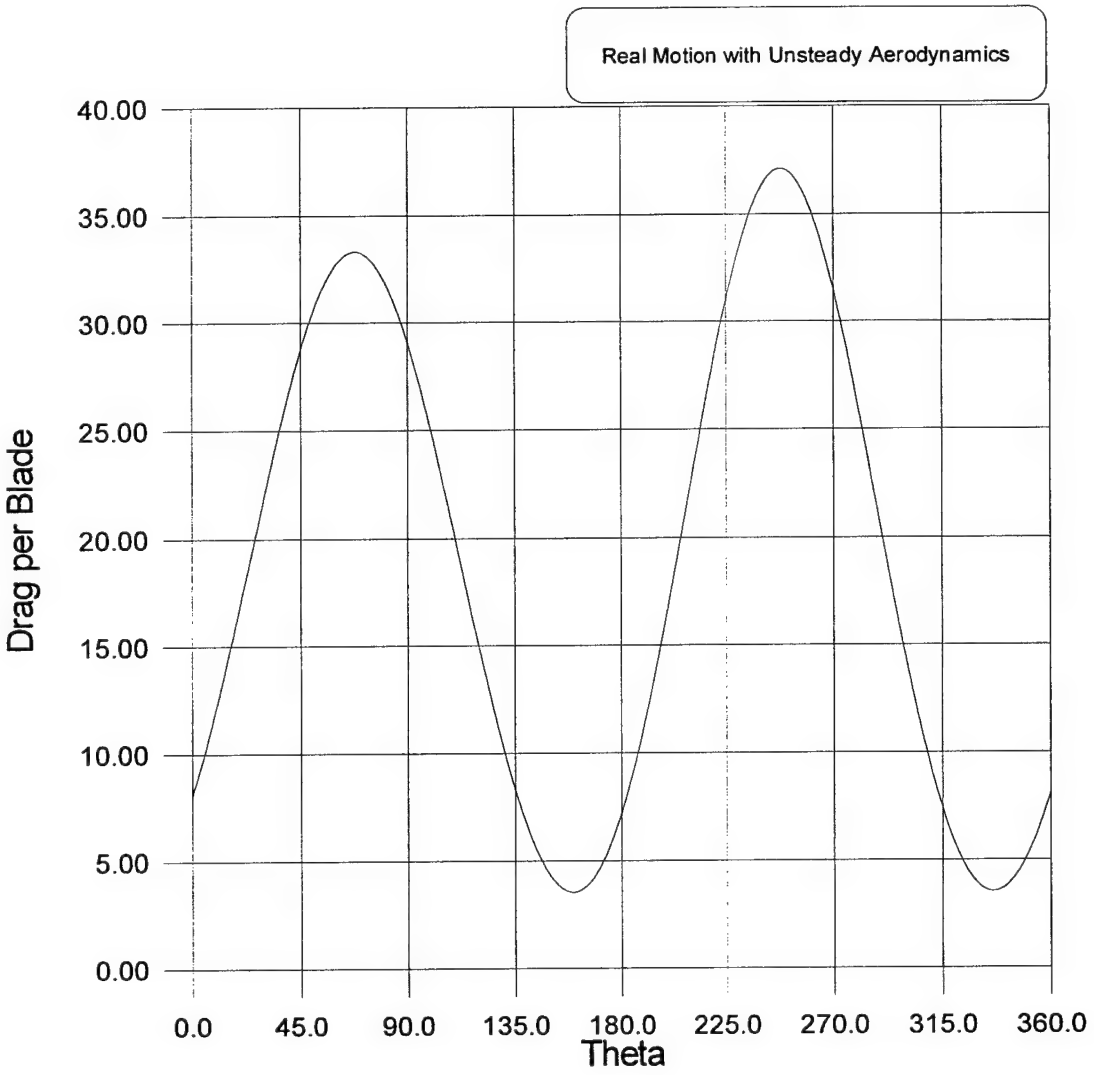

Six NACA 0012 Blades
650 RPM
Radius = 2 ft
Pivot Distance = 2.5 inches
8 lbs/Blade
Span = 4 ft
Chord = 1 ft
Offset = 1.03 inches
Phi = -32.78
Plot 6.

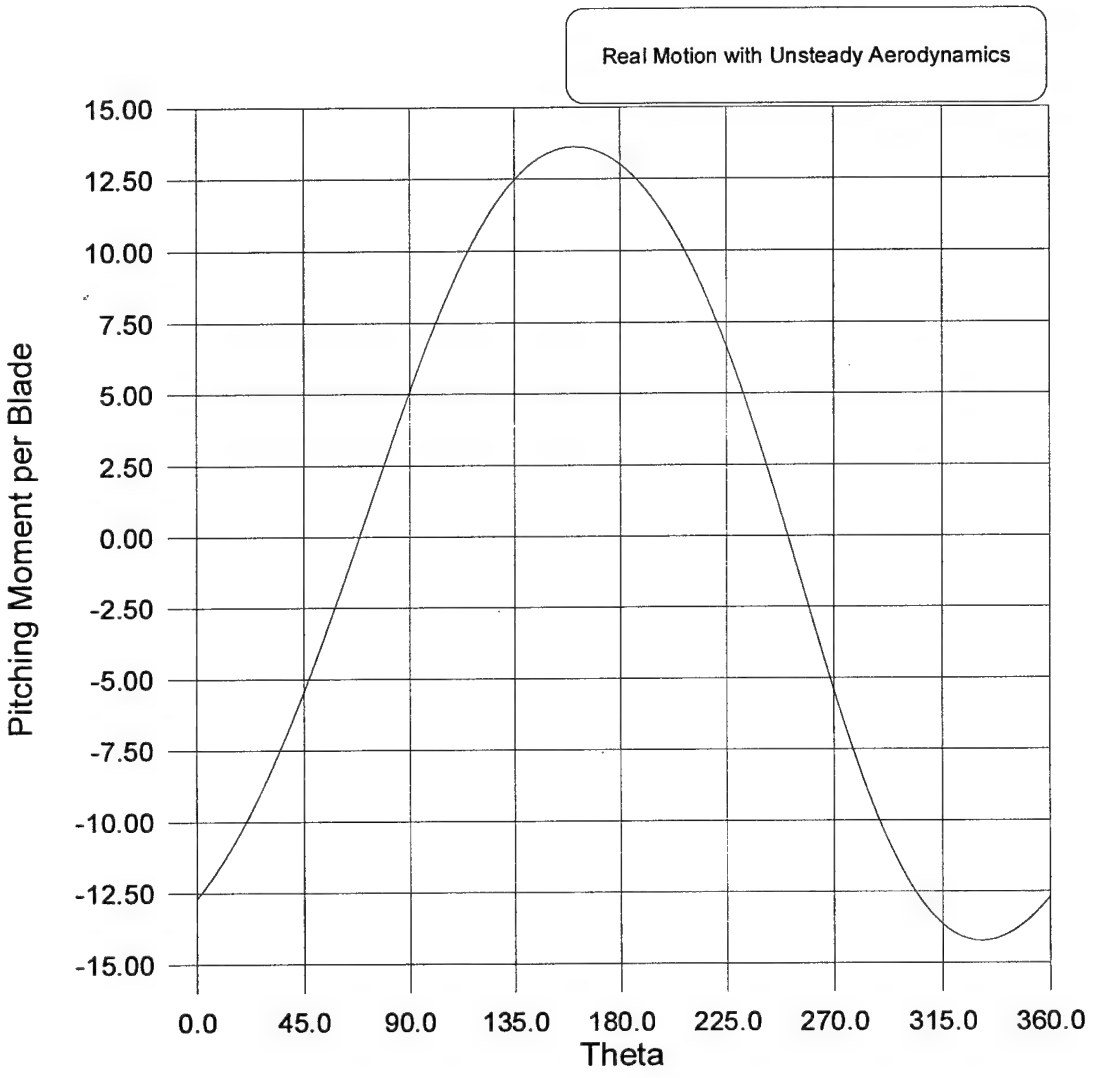

Six NACA 0012 Blades
650 RPM
Radius = 2 ft
Pivot Distance = 2.5 inches
8 lbs/Blade
Span = 4 ft
Chord = 1 ft
Offset = 1.03 inches
Phi = -32.78
Plot 7.

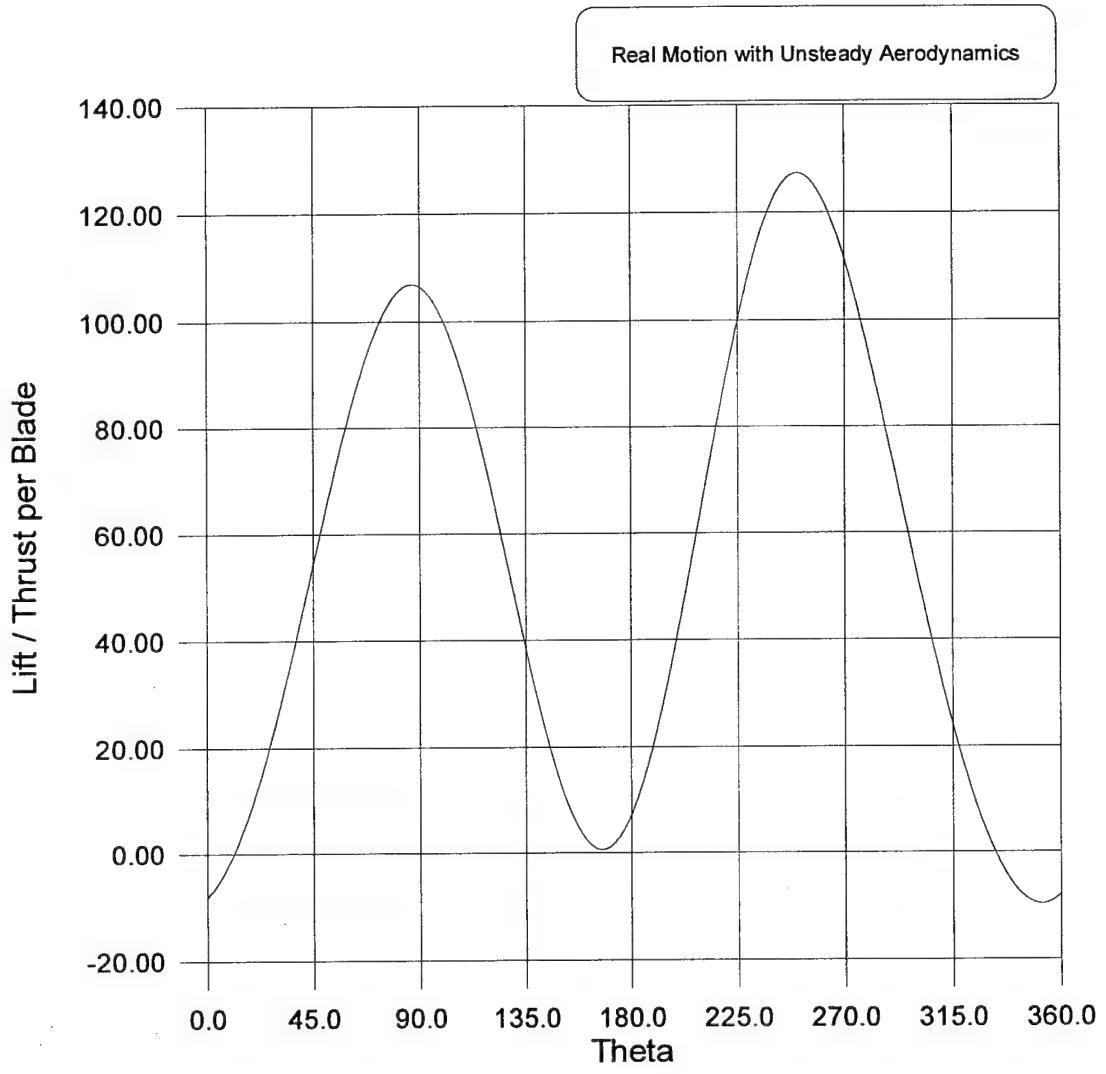

Six NACA 0012 Blades
650 RPM
Radius = 2 ft
Pivot Distance = 2.5 inches
8 lbs/Blade
Span = 4 ft
Chord = 1 ft
Offset = 1.03 inches
Phi = -32.78
Plot 8.

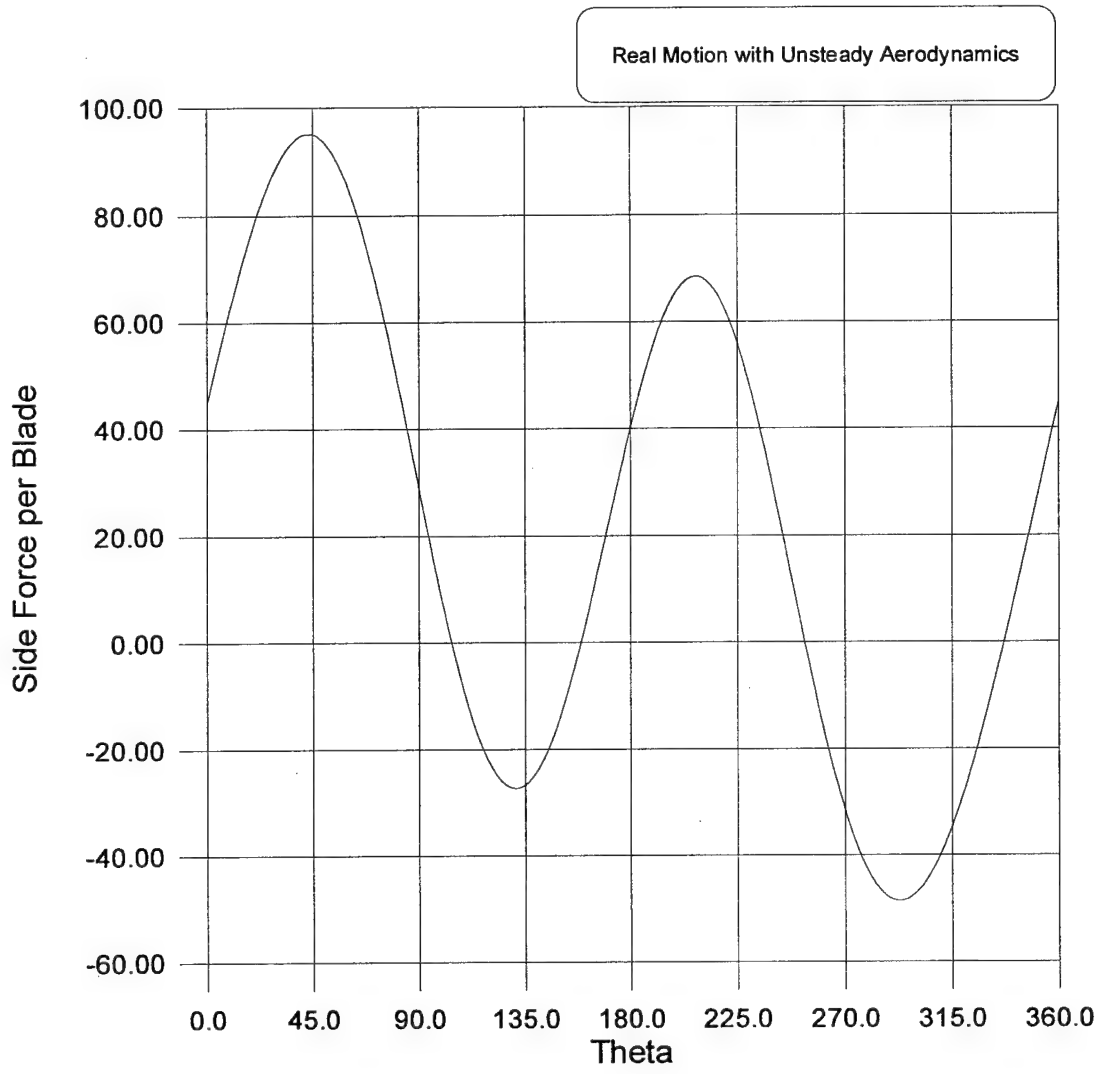

Six NACA 0012 Blades
650 RPM
Radius = 2 ft
Pivot Distance = 2.5 inches
8 lbs/Blade
Span = 4 ft
Chord = 1 ft
Offset = 1.03 inches
Phi = -32.78
Plot 9.

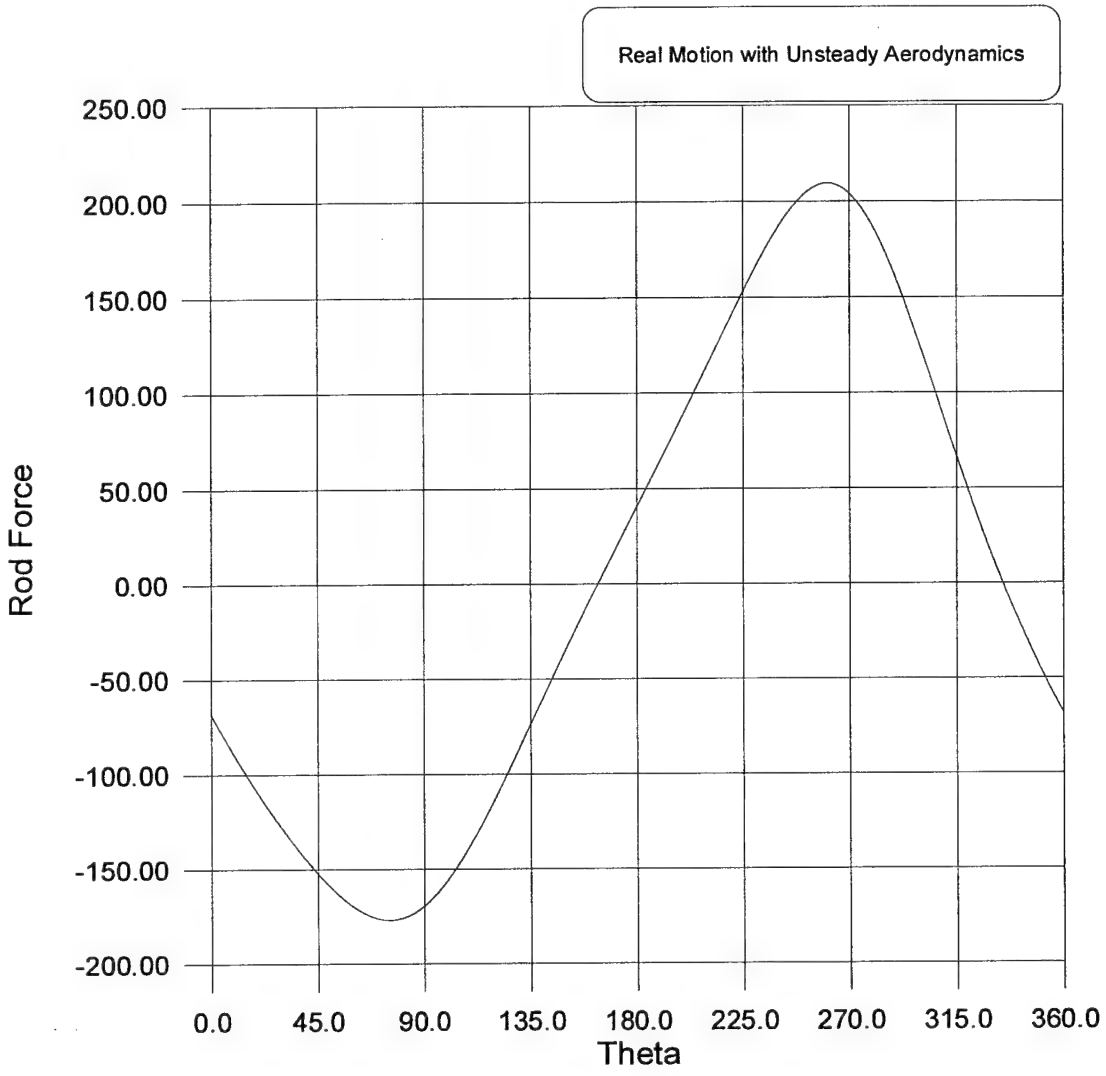

Six NACA 0012 Blades
650 RPM
Radius = 2 ft
Pivot Distance = 2.5 inches
8 lbs/Blade
Span = 4 ft
Chord = 1 ft
Offset = 1.03 inches
Phi = -32.78
Plot 10.

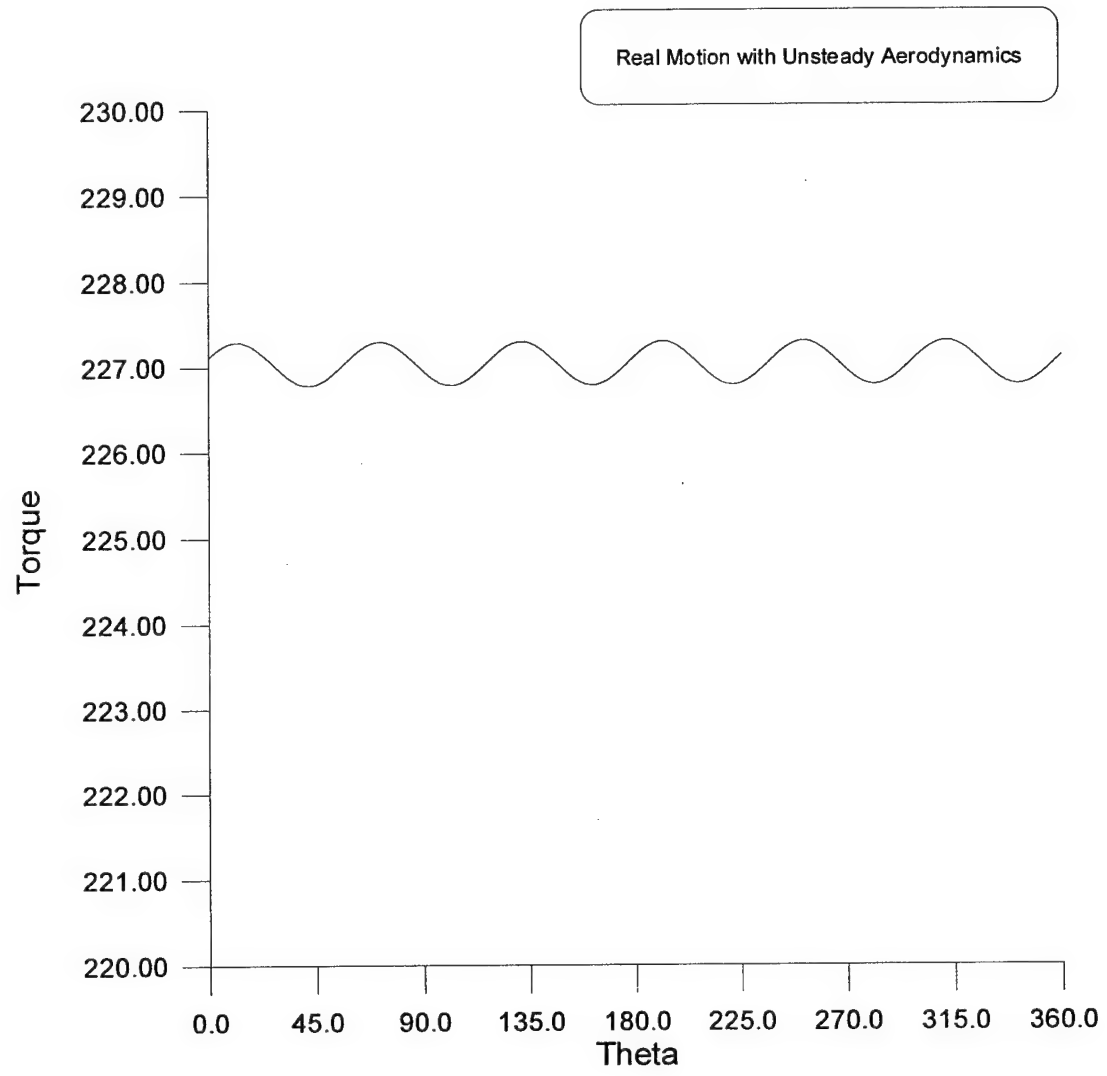

Six NACA 0012 Blades
650 RPM
Radius = 2 ft
Pivot Distance = 2.5 inches
8 lbs/Blade
Span = 4 ft
Chord = 1 ft
Offset = 1.03 inches
Phi = -32.78
Plot 11.

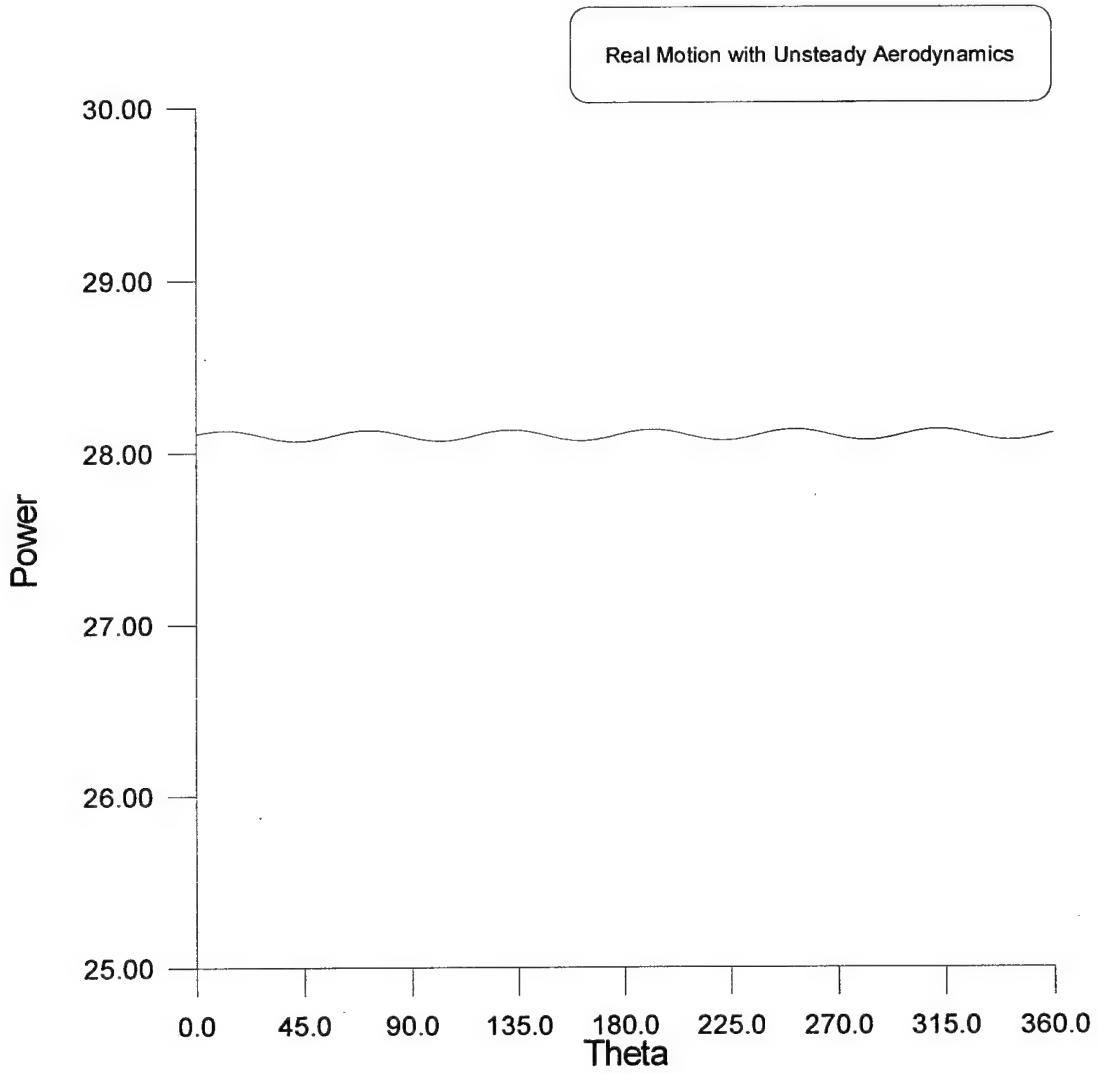

Six NACA 0012 Blades
650 RPM
Radius = 2 ft
Pivot Distance = 2.5 inches
8 lbs/Blade
Span = 4 ft
Chord = 1 ft
Offset = 1.03 inches
Phi = -32.78
Plot 12.

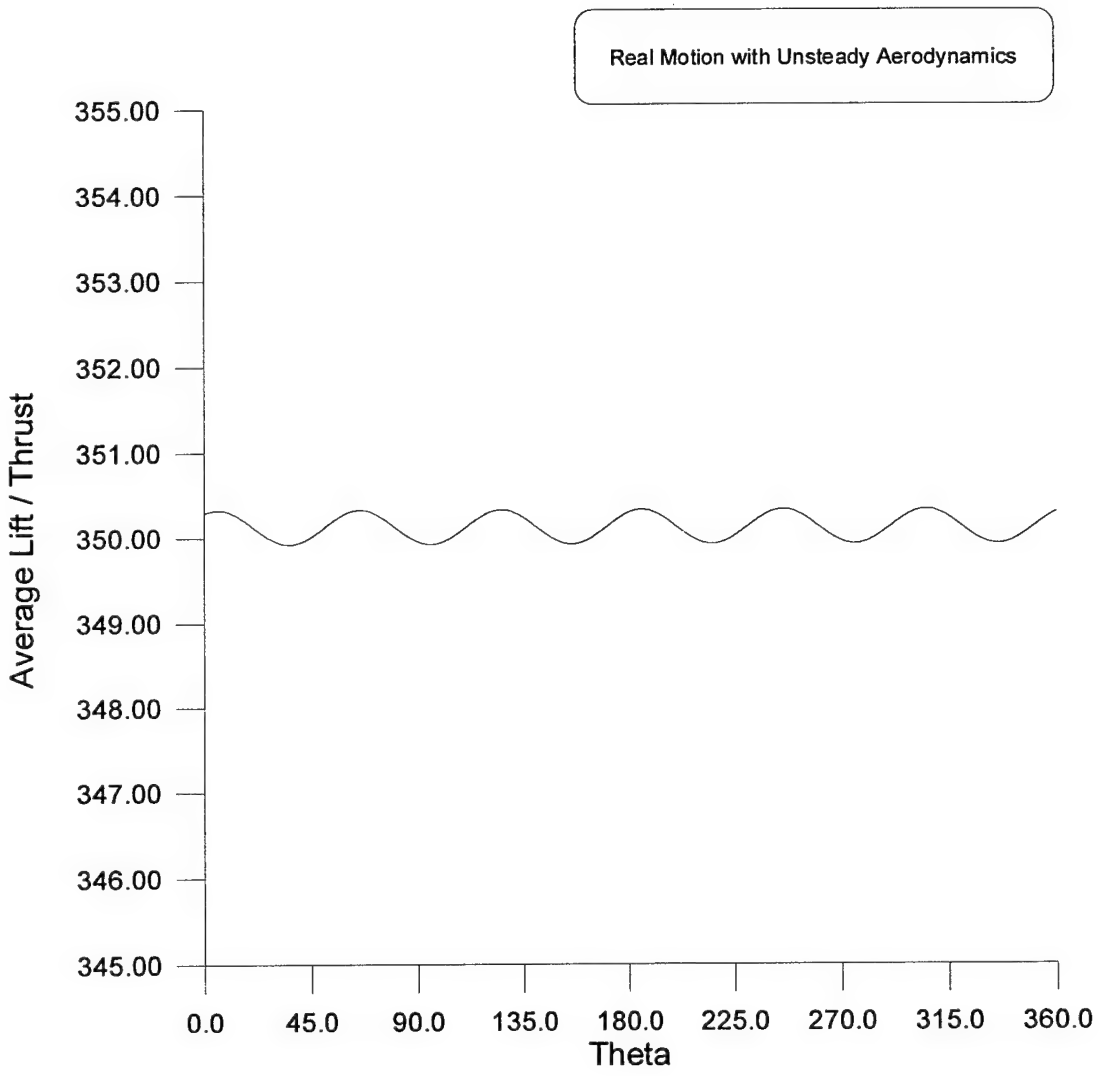

Appendix 2.

Plots of the Behavior of all Five Computer Programs

Six NACA 0012 Blades

650 RPM
Radius = 2 ft
Pivot Distance = 2.5 inches
8 lbs/Blade
Span = 4 ft
Chord = 1 ft
Plot 13.

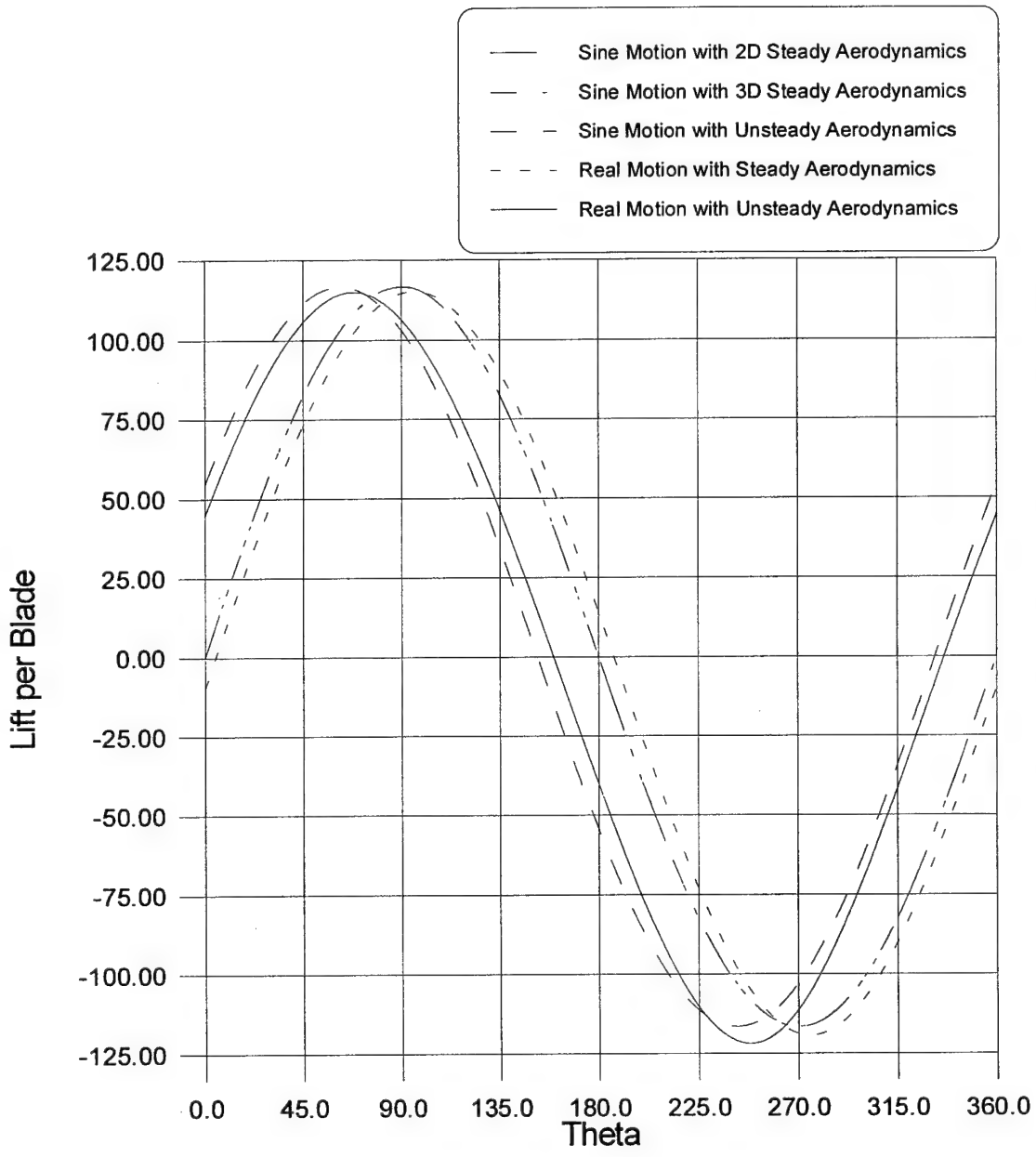

Six NACA 0012 Blades
650 RPM
Radius = 2 ft
Pivot Distance = 2.5 inches
8 lbs/Blade
Span = 4 ft
Chord = 1 ft
Plot 14.

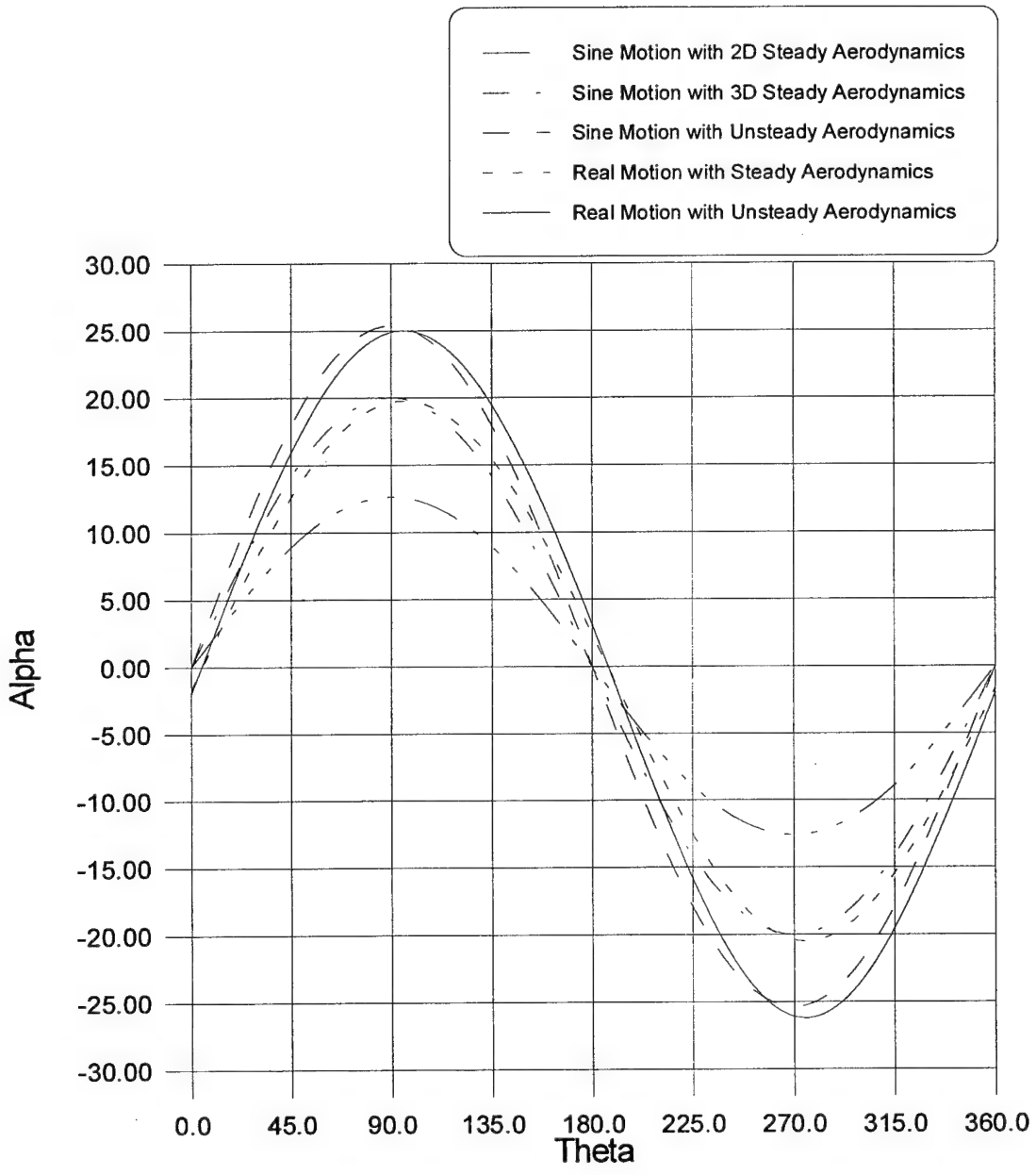

Six NACA 0012 Blades
650 RPM
Radius = 2 ft
Pivot Distance = 2.5 inches
8 lbs/Blade
Span = 4 ft
Chord = 1 ft
Plot 15.

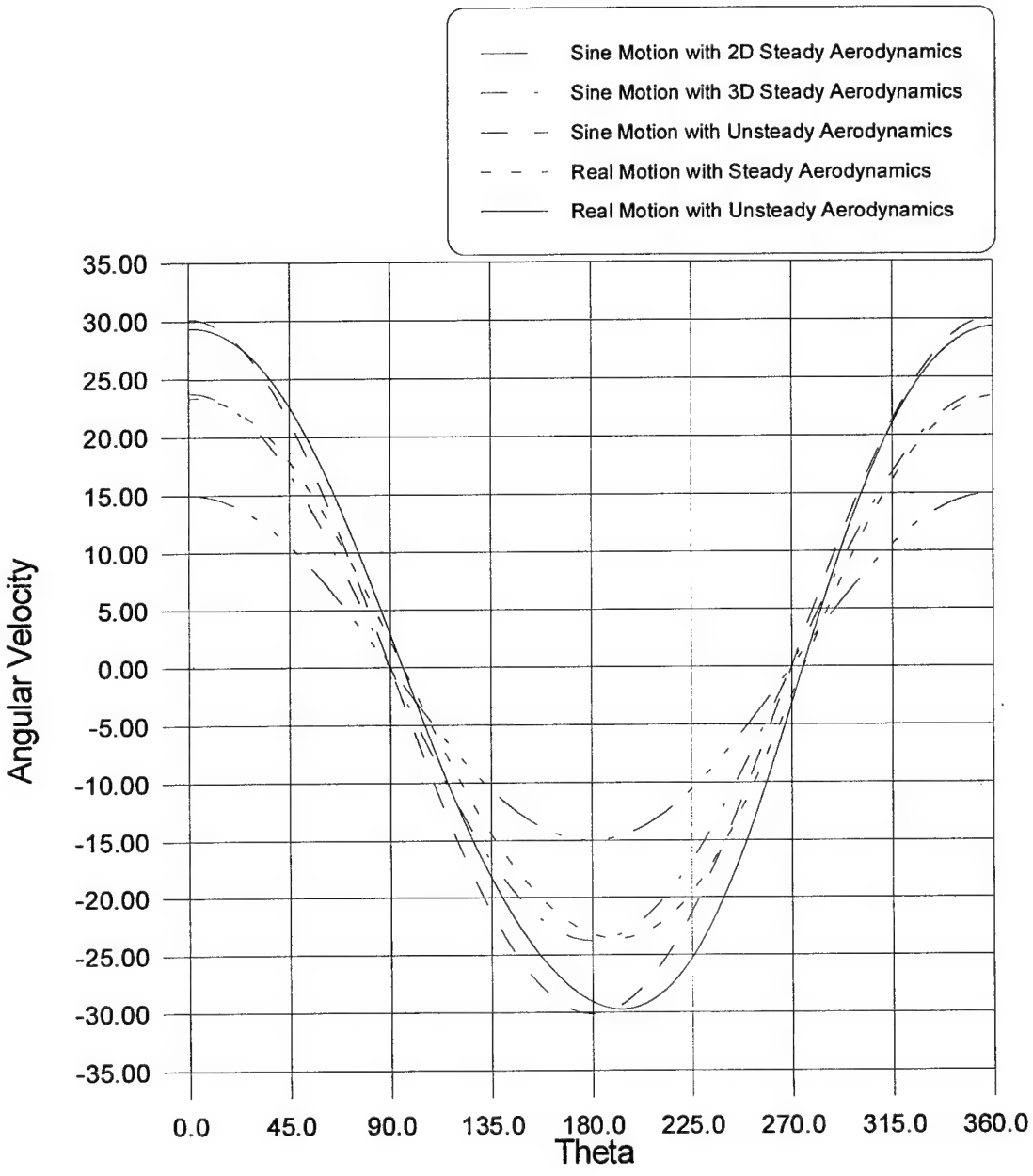

Six NACA 0012 Blades
650 RPM
Radius = 2 ft
Pivot Distance = 2.5 inches
8 lbs/Blade
Span = 4 ft
Chord = 1 ft
Plot 16.

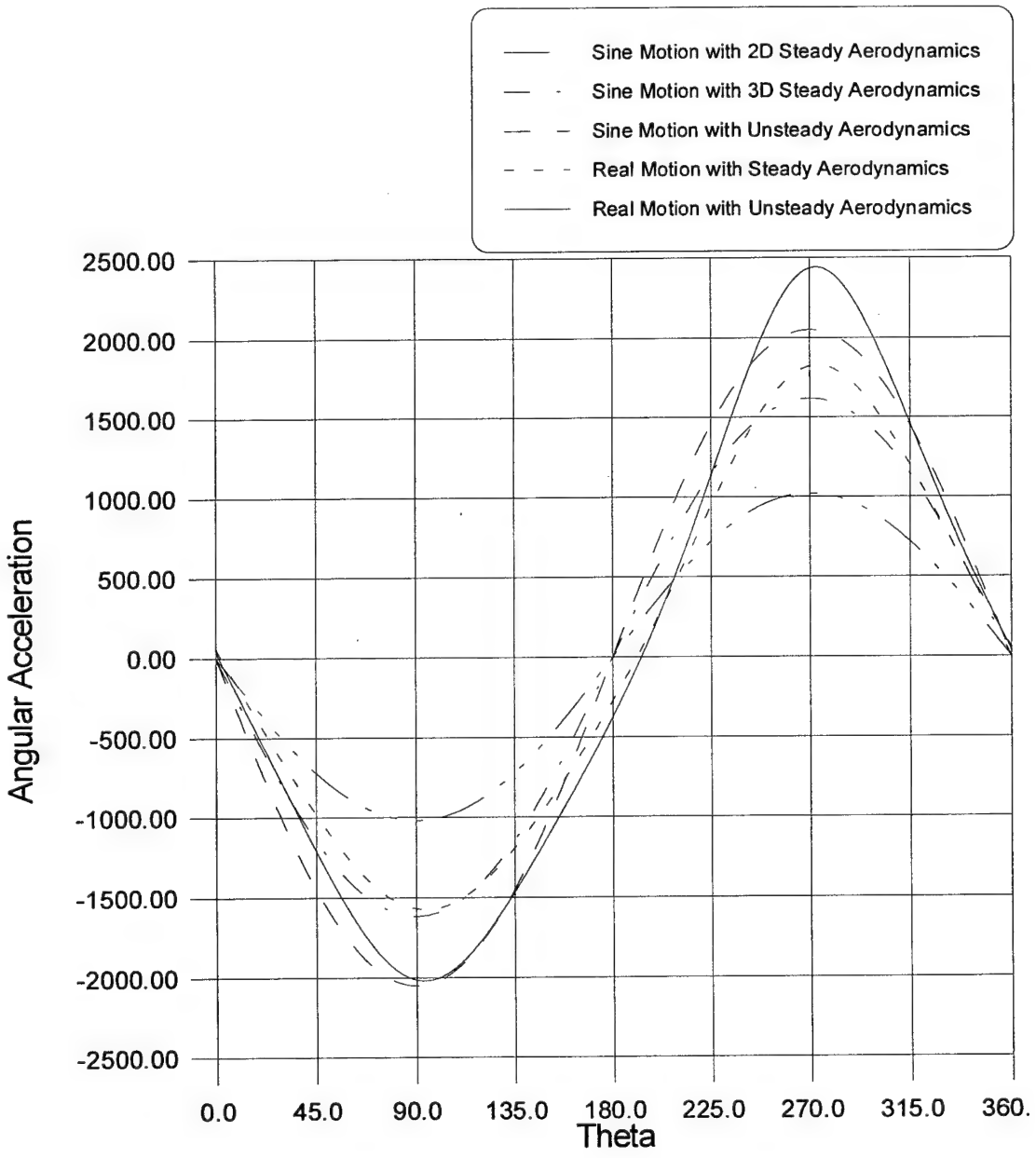

Six NACA 0012 Blades
650 RPM
Radius = 2 ft
Pivot Distance = 2.5 inches
8 lbs/Blade
Span = 4 ft
Chord = 1 ft
Plot 17.

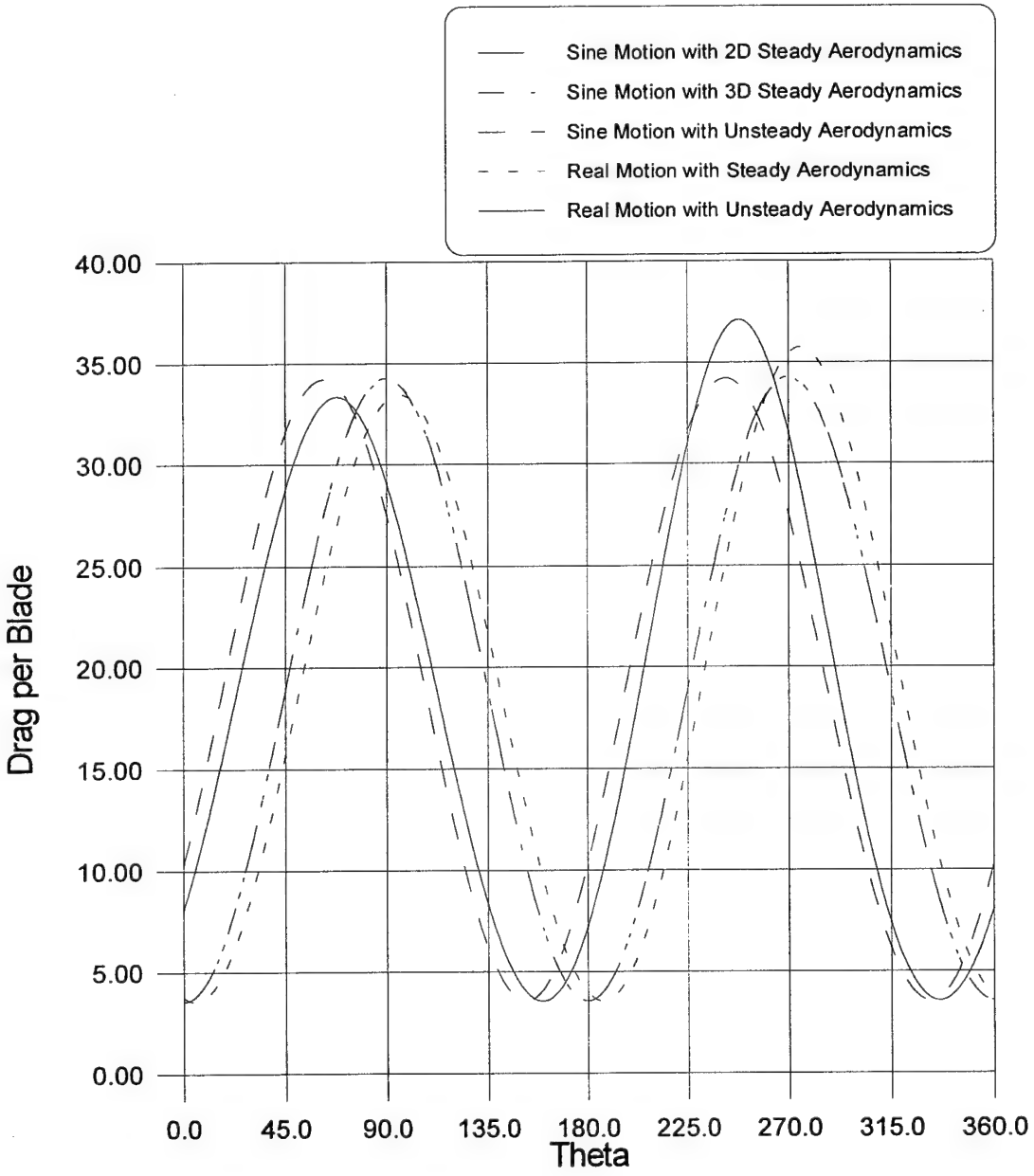

Six NACA 0012 Blades
650 RPM
Radius = 2 ft
Pivot Distance = 2.5 inches
8 lbs/Blade
Span = 4 ft
Chord = 1 ft
Plot 18.

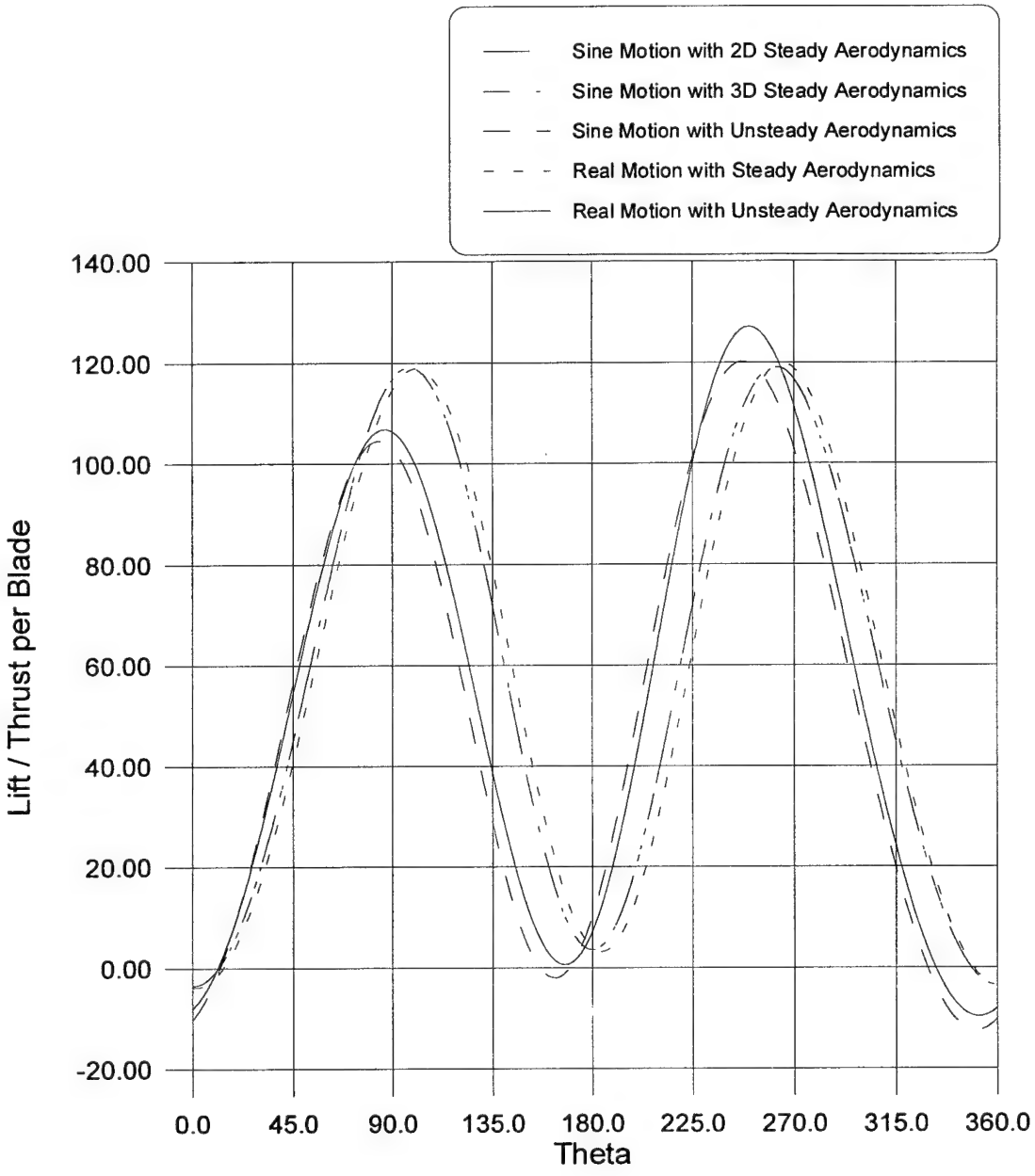

Six NACA 0012 Blades
650 RPM
Radius = 2 ft
Pivot Distance = 2.5 inches
8 lbs/Blade
Span = 4 ft
Chord = 1 ft
Plot 19.

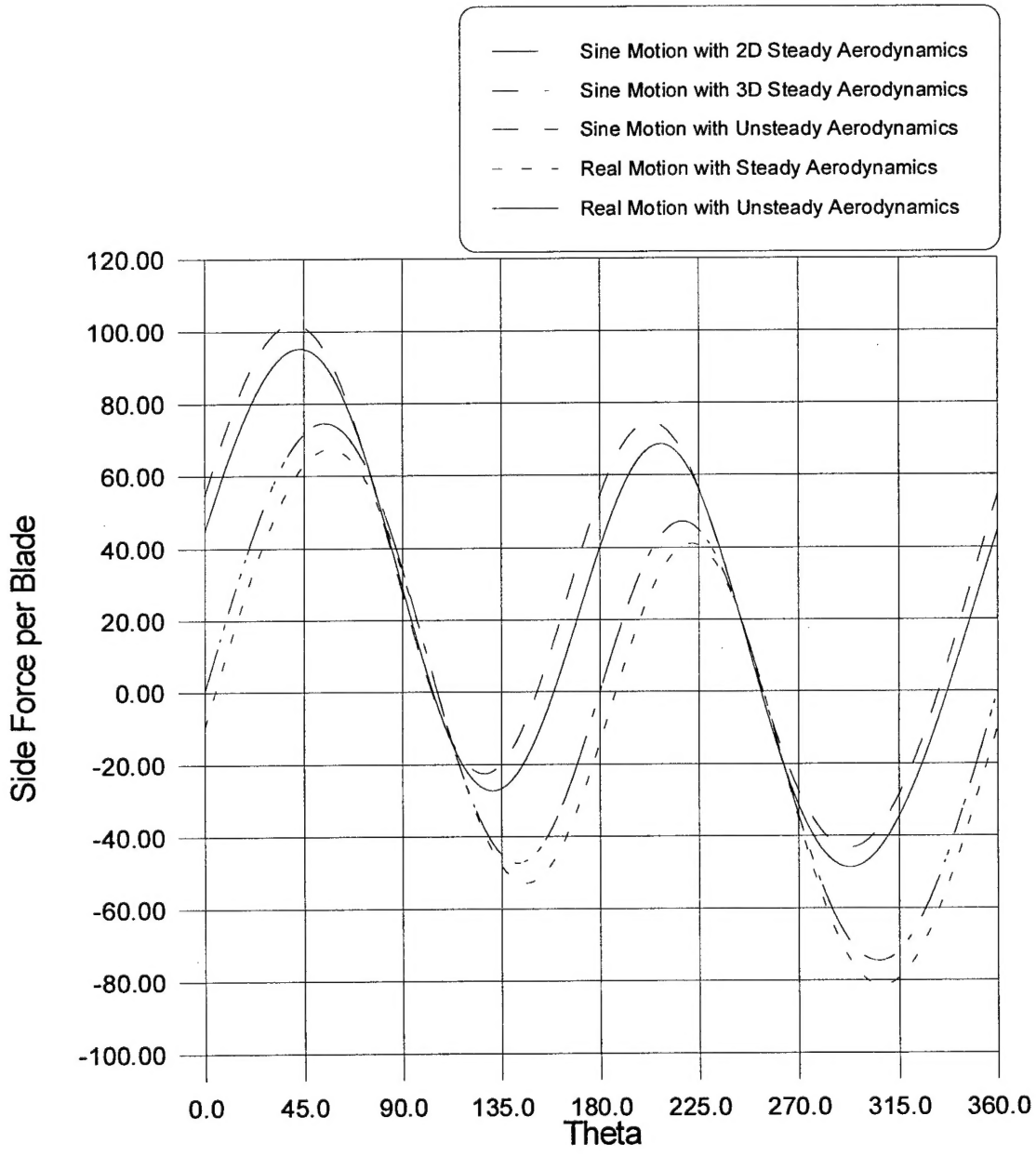

Six NACA 0012 Blades
650 RPM
Radius = 2 ft
Pivot Distance = 2.5 inches
8 lbs/Blade
Span = 4 ft
Chord = 1 ft
Plot 20.

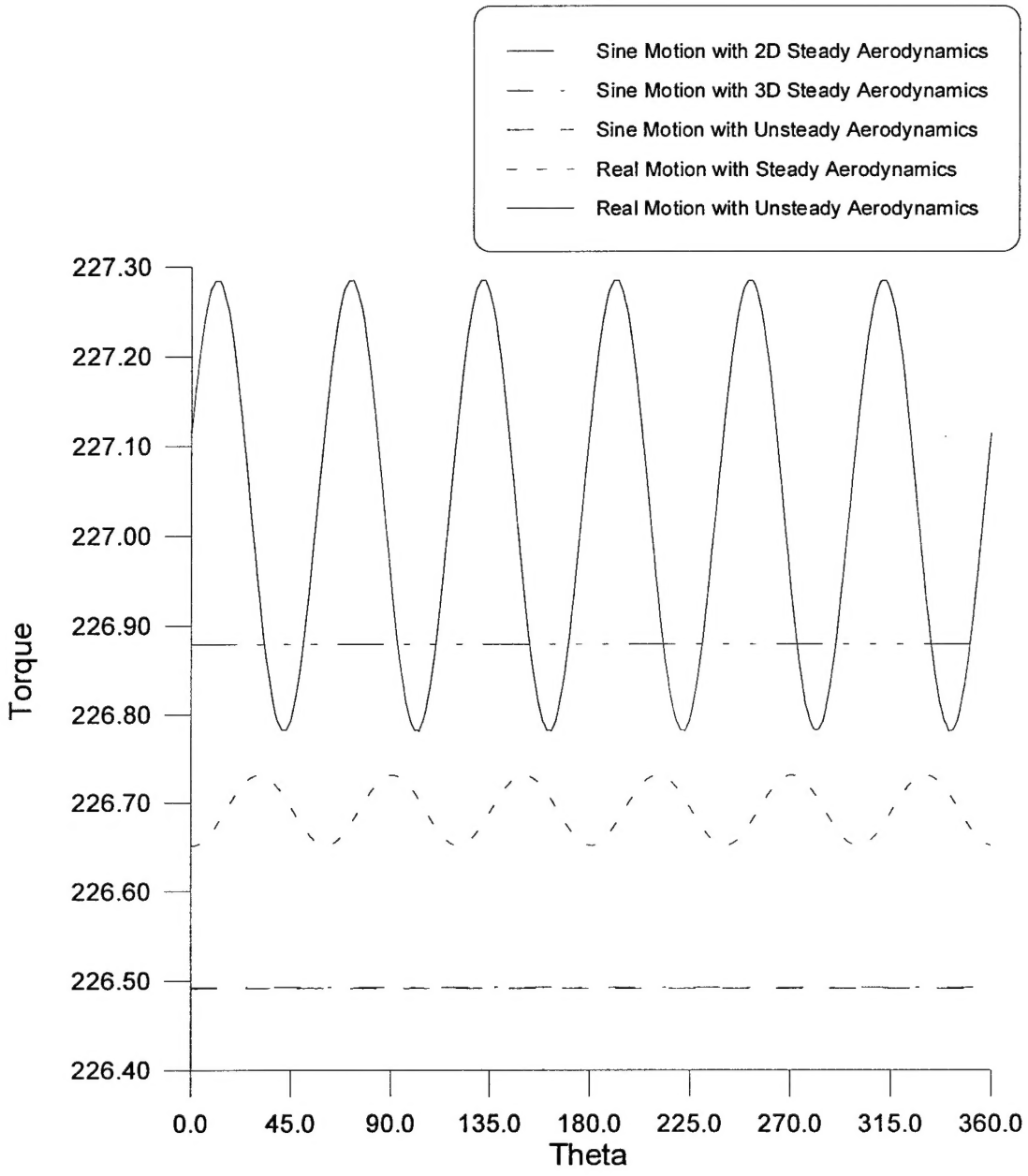

Six NACA 0012 Blades
650 RPM
Radius = 2 ft
Pivot Distance = 2.5 inches
8 lbs/Blade
Span = 4 ft
Chord = 1 ft
Plot 21.

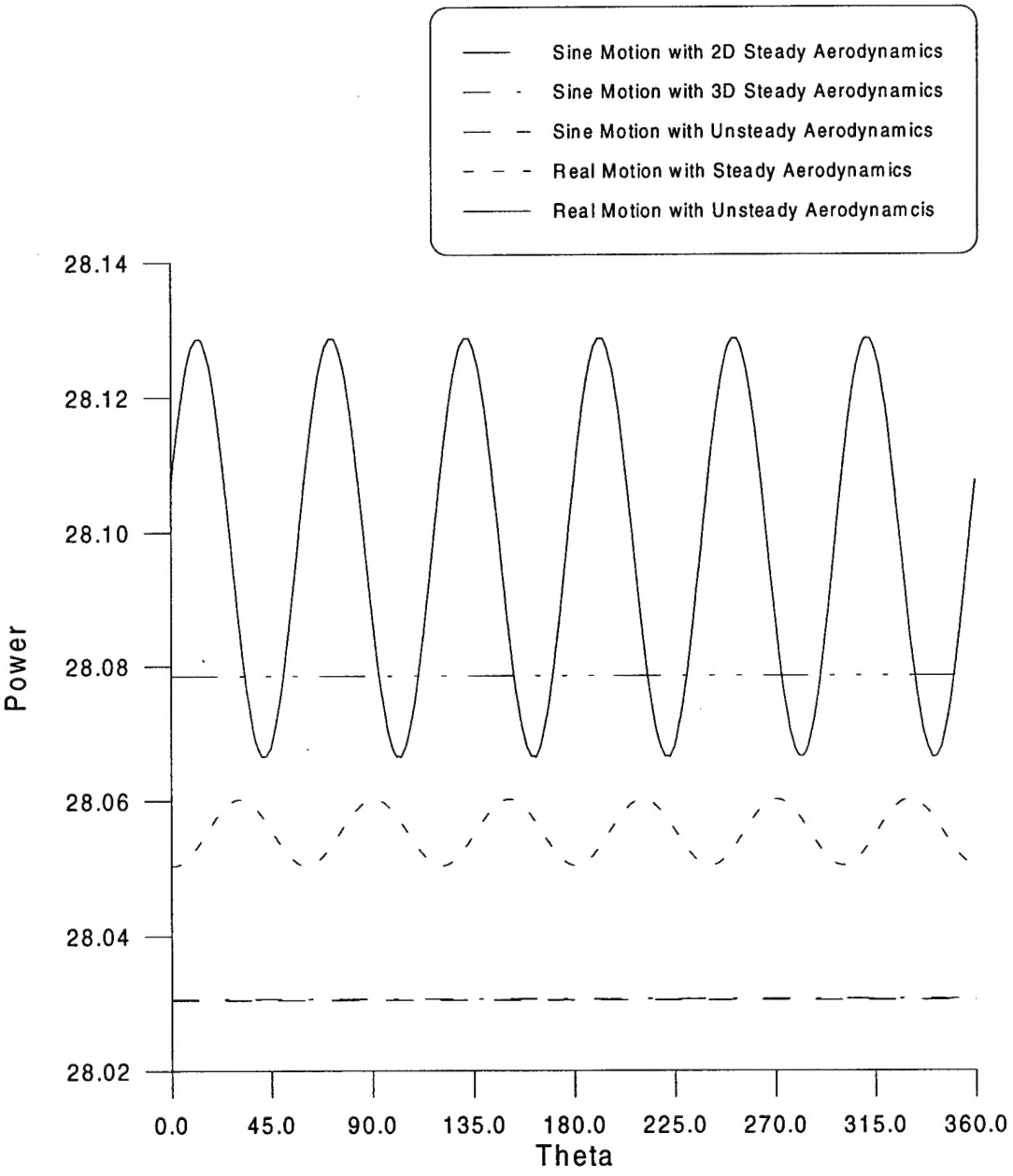

Six NACA 0012 Blades
650 RPM
Radius = 2 ft
Pivot Distance = 2.5 inches
8 lbs/Blade
Span = 4 ft
Chord = 1 ft
Plot 22.